CHAPTER 3

METHODOLOGY

In this chapter, the factors to be considered in the conceptual design of the proposed small-scale biomass solar power plant (BSPP), the analysis & equations required to develop the mathematical model, the installation of the solar parabolic trough collector at the Energy Park (EPC), and the subsequent collector testing & data measurement needed to validate the collector portion of the BSPP model, are described.

3.1 Design and Description of Proposed Solar Power Plant

As mentioned previously in Chapter 1, it is useful to have a mathematical model of a solar power plant system before proceeding to a detailed engineering design, construction & actual installation. However, in order to create the model, the basic layout of the proposed power plant has to be determined so that the necessary thermodynamic analysis can be carried out.

3.1.1 Conceptual Design of the Proposed Small-Scale BSPP

There are several factors to consider when designing for a solar thermal power plant irrespective of its final size and configuration. For a basic conceptual design of the proposed BSPP, some essential issues need to be considered:

(a) Consider: Output capacity (or size) of the power plant.

For a start, the nominal size of the power plant needs to be established. In this study, the size of the proposed BSPP is set at 20 kW_e (electric) in order to match the thermal output of the existing 50-m solar trough collector at the Energy Park (EPC), based on solar multiple SM = 1. (At the condition of SM = 1, there is no thermal energy storage since all the useful gain from the solar collector is used by the power block to produce electricity at the rated power). The rated power of 20 kW_e is determined, on first approximation, in the following manner. Based on the average hourly direct radiation $I_{s,s}$

of 700 W/m^2 calculated for Phitsanulok for sunny condition (refer to section 3.3.2), and assuming an overall solar-to-electric efficiency η_{total} of 11.5% (which is the mid value of the average 9–14% range reported by Escalante (1998) [16]), the power output P_{rated} from the 50-m EPC (with 240 m^2 of aperture area) is calculated to be 19.32 kW$_e$ (using equation (3.27), and replacing η_i with η_{total} & Q_u with P_{rated}). In this study, the approximated value of 19.32 kW$_e$ is rounded up to 20 kW$_e$ for practical reason & convenience. Other factors that may influence the design-size of a power plant include: the load demand, available land area, and available capital. However, these factors will not be discussed in this study.

(b) Consider: Type & source of input energy.

A solar thermal power plant based on CSP technology can function only with direct radiation and is usually considered for locations with an annual direct irradiation of at least 1700 kWh/m^2.a [33]. Under the insolation condition of Thailand, it is not effective to operate a solar thermal power plant entirely on solar energy due to the presence of a relatively high diffuse radiation fraction. To operate such a power plant, another energy source is needed as a backup. Hence, to make good use of the locally available solar and biomass resource potential, the proposed BSPP is conceptually designed to utilize solar energy as the primary input source & biomass energy as the backup source (Figure 14).

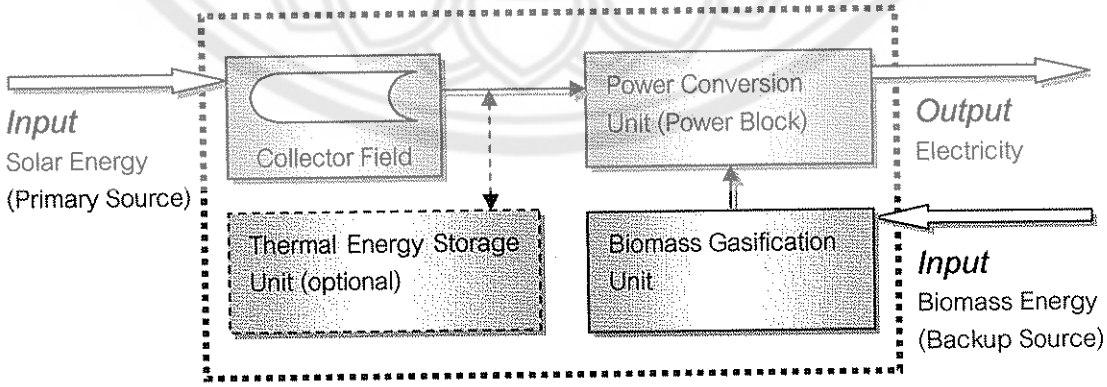

Figure 14 Overall flow and energy transfer of the proposed BSPP

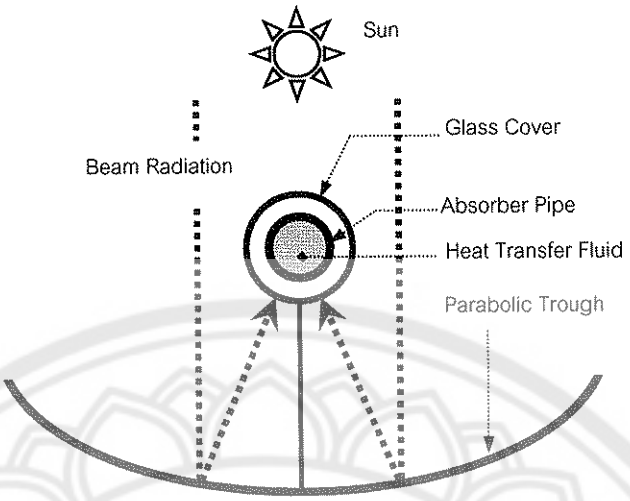

Figure 15 Section of a parabolic trough concentrator

(c) Consider: Method of energy collection & conversion.

In the proposed BSPP, parabolic trough technology is used for solar energy collection & concentration (Figure 15), and biomass gasification technology is used to convert agricultural residues into producer gas for combustion. As mentioned in Chapter 2, parabolic trough collector is the most mature of all the CSP technologies with low technical risk, and is most suited to operate in the temperature range of 100-400 °C. Biomass gasification is superior to direct combustion because the producer gas can burn more cleanly & efficiently than the solid biomass fuel it is derived from.

(d) Consider: Type of heat transfer medium.

The proposed BSPP is designed to operate with a collector field that uses thermal mineral oil as the heat transfer medium. Such a design will allow for the easy integration of a thermal energy storage system with the collector field. Besides, the local insolation conditions also favor an oil-based collector system since the operating temperature is not expected to exceed 300 °C. As mentioned in Chapter 2, the full advantage of direct steam generation (DSG) is realized only if the collector can operate at or close to 550 °C & 100 bar. In addition, the generally higher operating temperature & pressure needed for the DSG process would make construction, operation & maintenance of the power plant relatively more difficult & demanding.

(e) Consider: Type of power cycle and prime mover.

A solar power plant with trough collector necessitates the use of a Rankine steam cycle for the power block. The prime mover (or engine) can either be a steam turbine or steam piston engine. A steam turbine operates best with superheated or dry steam. Saturated or wet steam tends to damage the blades of the turbine. On the other hand, a steam piston engine is more robust and can operate well with both dry and wet steam. A piston engine can be easily fabricated from parts of a car engine and generally cost less than a similar-size turbine. Although a well-designed turbine may be more efficient than a piston engine, the efficiency tends to decrease with reducing turbine size [34]. This makes its comparative advantage less obvious at low capacity. Hence, it may be more cost-effective to use a piston engine in small power systems, particularly for those in the kilowatt range. Almanza & Lentz (2001) reported the production of electricity at low powers using parabolic trough collectors coupled to a 2.24 kW (3 hp) two-piston steam engine that operated with saturated steam at 165 ^{o}C and 7.0 bar pressure [30]. Figure 16 shows the picture of a four-piston steam engine that was modified from parts of a conventional car engine and which can be assembled locally in Thailand. In this study, a steam piston engine is suggested as the prime mover in the proposed power plant in view of the reasons mentioned above.

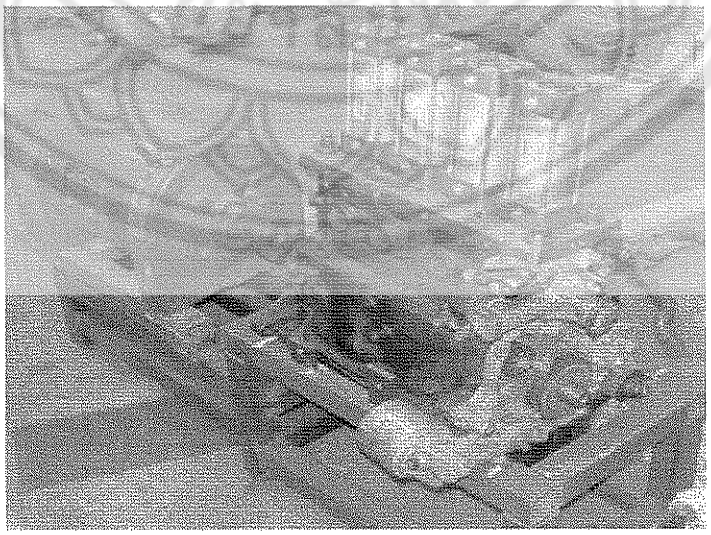

Figure 16 A 4-piston steam engine coupled with generator

(f) Consider: Operation under different weather conditions.

The proposed BSPP is envisaged to operate under three possible weather scenarios: sunny, partly cloudy and fully cloudy conditions. In this study, "sunny" denotes the solar insolation of a location under the condition of standard "clear sky radiation"; whereas "partly cloudy" denotes the insolation of the same location under the condition of "average radiation"; while "fully cloudy" indicates no direct radiation is available. The methods to estimate the direct radiation based on "clear sky radiation" and "average radiation" conditions are described in section 3.3 of this chapter.

(g) Consider: Type of thermal energy storage system and storage capacity.

As mentioned in Chapter 2, sensible heat storage using thermal mineral oil is currently the most economical method for operating temperatures of up to 300 °C [28]. In this study, a hot tank/cold tank system capable of providing at least 6 hours of thermal storage using mineral oil as storage medium is used to extend the generation capacity of the power plant. Although the capital cost of a single-tank thermocline system may be lower than a two-tank system, a perfectly stable thermocline is not easy to achieve in practice. Also, the discharging temperature from a single-tank thermocline tends to decrease with time, while that from a two-tank system is able to remain constant during discharging. This is significant since a constant exit temperature implies that the load stream flowrate can remain constant and electricity can be produced at a steady rate. Furthermore, a two-tank system can be very useful during maintenance & repair with the second tank functioning as a reservoir & drainage tank in the event of a leak. However, it should be remembered that thermal energy storage (TES) is optional. In reality, its inclusion in a BSPP-type power plant is mainly a matter of economics.

(h) Consider: The start, end and duration of daily operation.

The proposed BSPP is conceptually designed to operate from 08:00 am to 16:00 pm for an 8-hour operation-day. However, in actual practice, the power plant is likely to startup at least one hour earlier so that near-steady conditions can be achieved by the start of the operation-day. In addition, thermal energy storage & biomass backup energy can be incorporated to increase the generation capacity of the power plant.

3.1.2 Description of the Proposed Small-Scale BSPP

After considering the issues mentioned above and establishing the relevant design requirements, the next step is to define a basic layout for the proposed BSPP. *Importantly, it must be remembered that the purpose of this study is not to create a detailed design of a power plant with full engineering specifications. But rather, it is an initial study to introduce the concept of a BSPP and to develop a simplified model of it, so that future research may build on this work and design a real-life power plant eventually.* Hence, the design of the BSPP used in this study shows only the basic layout that is sufficient for a thermodynamic analysis to model the main energy transfer & conversion processes that take place in the power plant system.

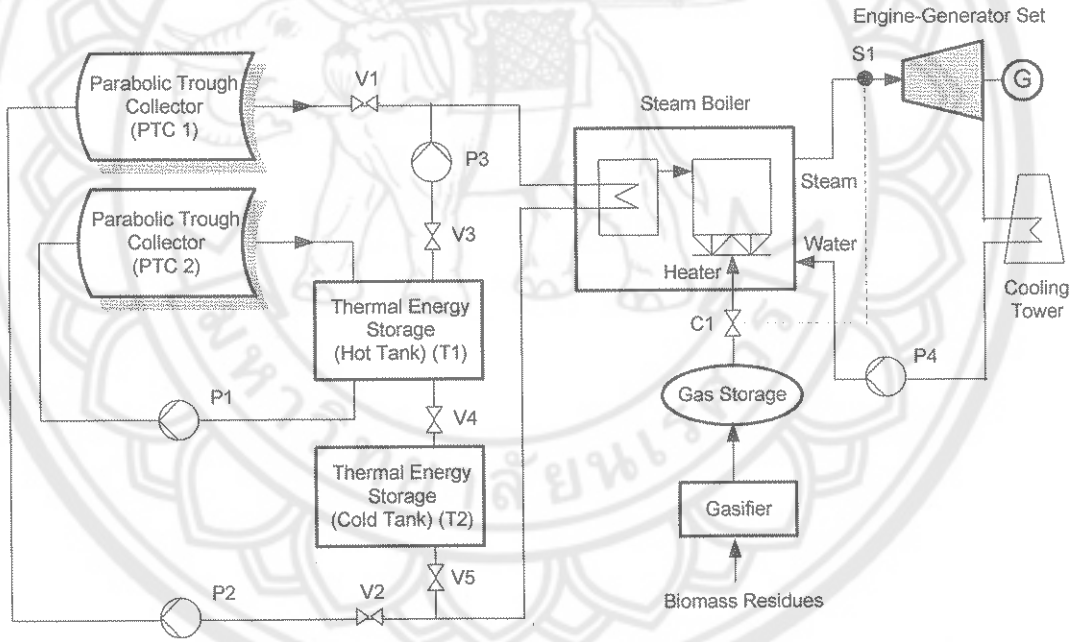

Figure 17 Basic layout of a small-scale biomass solar power plant (BSPP)

The basic layout of the proposed BSPP is shown in Figure 17. It is made up of four major sub-systems as follow:

(a) A collector field to collect and convert solar energy into thermal energy.

The collector (or solar) field is consisted of two 50-m long parabolic trough collectors (PTC 1 & PTC 2). The aperture width & length of each collector is 5 m & 48 m respectively, giving a total aperture area of 240 m^2 per collector. The heat collecting element (or receiver), located at the focus of the parabola, is consisted of a cylindrical absorber enclosed within a glass pipe. A heat transfer fluid (thermal mineral oil) flows through the inside of the absorber pipe. Both PTC 1 & PTC 2 are located in separate loops. PTC 1 is in the loop that is linked to the Rankine steam cycle via the steam boiler, whereas PTC 2 is in the loop that is connected to the thermal energy storage tank (T1).

(b) A thermal energy storage unit.

The thermal energy storage (TES) unit is consisted of two insulated stainless steel tanks, each having the capacity to hold an amount of oil that is capable of providing at least 6 hours of thermal storage. The tanks are divided into hot tank (T1) and cold tank (T2). The hot tank is connected to the outlet of collector PTC 2, while the cold tank is connected to the inlet of collector PTC 1.

(c) A biomass gasification unit with gas storage.

The biomass gasification system is consisted of a reactor, gas cleaning unit, hopper, conveyor feeding unit, gas storage tank, and gas heater. The reactor is a fixed-bed, downdraft, throatless, open-top gasifier which is suitable for gasifying rice husk. (Rice husk is one of the most available agricultural residues in Phitsanulok province and is the example used in this study). The gas cleaning unit is a dry cleanup system consisting of a high temperature char/ash coarse settler and a high efficiency cyclone separator. The cleaned gas is piped to the heater of the steam boiler via a gas storage tank. The capacity of the storage tank is enough to compensate for the startup time of the gasifier so that instant energy supply to the steam boiler is always available. Calculation of the minimum volume of the gas storage tank is given in section 3.4.2.

(d) A power conversion unit (PCU) or power block.

The fourth sub-system of the power plant is the power conversion unit (PCU) or power block. The PCU operates on the principle of a Rankine steam cycle and is consisted of a steam boiler, piston engine-generator set, condenser, and pump. The steam boiler contains an oil-water heat exchanger and a gas heater. Any energy deficit in the heat exchanger is compensated by the energy input from the gas heater which is fired by the producer gas from the biomass gasifier. The prime mover is a reciprocating 4-piston steam engine modified from a conventional car engine. It operates at a maximum rpm of 900 and is coupled to an electric generator which produces electricity at the rated power of 20 kW_e. The condenser is a cooling tower which can be dry or wet.

The proposed BSPP is envisaged to operate in three possible weather scenarios: sunny, partly cloudy and fully cloudy. On a typical operation-day, the power plant is expected to operate from 08:00 am to 16:00 pm. The operation of the power plant under each weather condition is described in the following section.

(i) Operation during sunny condition.

During sunny condition, the power plant functions in a "solar" mode. This means that the thermal output from the collector is sufficient to meet the full demand of the power block and the power plant is able to generate electricity at its rated power. In normal operation (referring to Figure 17), valves V1 & V2 open to allow the heat transfer fluid (oil) to flow through collector PTC 1, while valves V3, V4 & V5 are closed. At the same time, pumps P1, P2 & P4 are switched on and pump P3 remains off. The hot oil exits from PTC 1 and passes through the steam boiler where steam is produced to operate the engine-generator set. In a separate loop, HTF is simultaneously heated by collector PTC 2 to charge the storage tank T1. Once the storage medium (oil) in T1 attains the desired maximum storage temperature, pump P1 deactivates and collector PTC 2 stops tracking the sun. When tank T1 is fully charged, it can extend the operation time of the power block when the collector field shutdown after 16:00 pm. At this time, valves V1, V2 & V4 are closed, while valves V3 & V5 open to allow the hot oil from tank T1 to flow through the steam boiler. At the same time, pumps 1 & 2 are switched off and

pumps 3 & 4 are activated. Then the oil exits the steam boiler and returns to tank T2 to be stored. When all the hot oil from tank T1 has passed through the boiler & transferred to tank T2, the discharging process stops. Then valve V4 opens to allow the oil in tank T2 to return to tank T1 where it awaits another round of thermal charging the next day.

(ii) Operation during partly cloudy condition.

During partly cloudy condition, the power plant functions in a "hybrid" mode. This means that the thermal output from the collector is insufficient to meet the full demand of the power block and the power plant is unable to generate electricity at its rated power. In this case, the gas heater fires to provide more heat to the steam boiler to compensate for the energy deficit. Sensor S1 monitors the conditions of the steam at the inlet of the engine-generator and the signal is feedback to control valve C1 to adjust the gas flow rate accordingly. Thus, by using biomass energy in addition to solar energy, the power plant is now able to generate electricity at its rated power. However, with regards to thermal energy storage, it is possible that tank T1 cannot be charged to its full capacity since the desired maximum storage temperature may be unattainable.

(iii) Operation during fully cloudy condition.

During fully cloudy condition, the power plant functions in a "biomass" mode. This means that no useable solar energy is available and the power plant has to depend solely on biomass energy to generate electricity at its rated power. In this case, thermal energy storage is not possible.

3.2 Development and Explanation of Mathematical Model

3.2.1 Characteristics (uniqueness) of the BSPP Model

The mathematical model of the BSPP is developed based on the four sub-systems of the proposed power plant introduced in section 3.1. Each sub-system corresponds to one segment or sub-routine of the overall power plant model. The BSPP model can then be used, in conjunction with the solar radiation (SR) model (section

3.2.6), as a tool for performance analysis and parametric study (Figure 18). In the course of developing the BSPP model, the general guideline of using "*logical algorithm, appropriate equations and reasonable assumptions*" is followed as far as possible.

In this study, Excel Spreadsheet is the preferred development software tool used to encode all the equations of the model because of the following reasons: (a) All the changes in sun angles & fluid properties are evaluated on an hourly time-interval basis corresponding to the changes in solar radiation; Excel software can handle this effortlessly, thus avoiding the loops & iterative steps needed by other development tools, (b) There are not many requirements for iteration in the BSPP model; iteration is usually avoided whenever it is deemed unnecessary, (c) Linear & curvilinear regression techniques are used in the BSPP model; Excel software has a built-in feature that can perform this task effectively, (d) Exactness in the quantitative results is not the emphasis of the BSPP model; rather, the qualitative aspect of the results is more useful & instructive. (In this study, the use of approximated results is sufficient to indicate important trends & implications in all cases), and (e) Most people are familiar with the Excel software than with other development tools, thus making the BSPP model more accessible & user-friendly.

At this juncture, it should be emphasized that the BSPP model created in this study is not meant to function as an optimization program by itself. Rather, it is an analytical tool that is capable of system performance simulation and parametric study, and which can be used for optimization analysis if required. In general, the characteristics or unique features of the BSPP Model can be summarized as follow:

(a) It is formulated based on standard, uncomplicated thermodynamic equations.

(b) It has a simple structure and is easy to understand.

(c) No special computing skill is needed to use the Model.

(d) It is developed using Excel Spreadsheet for easy access by most users.

(e) It can cater to the basic needs of students & researchers in the field of solar thermal technology.

(f) It can be useful in pre-feasibility studies where quick estimates of energy performance are helpful.

A description of each sub-routine is given in the following section beginning with the collector system (CS) model, which is considered to be the most important part of the BSPP model.

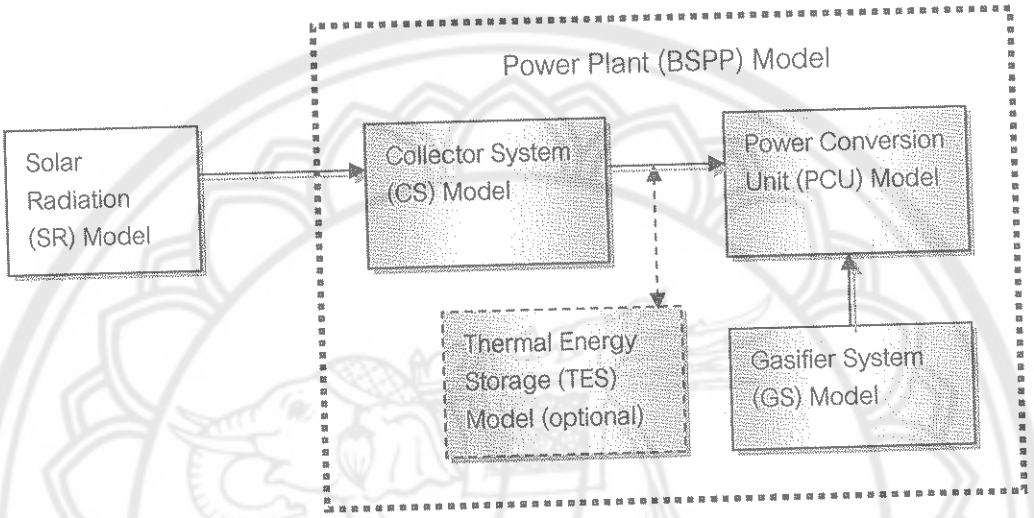

Figure 18 Block diagram of a BSPP mathematical model

3.2.2 Collector System (CS) Model

The collector system (CS) model is the most critical segment in the entire BSPP model because the input values of the other components (i.e. gasifier, TES unit & PCU) in the power plant model are totally dependent on the output values of the collector. Unlike a gasifier where the energy conversion is predictable and based mainly on the conversion factors of the fuel, a collector converts solar energy which varies in quality & magnitude with respect to time. *Essentially, this means that once the collector system model has been appropriately formulated and validated, the thermal performance for the rest of the power plant can be defined, thus implying the validation of the power plant model, as a whole, as well.*

There are many input variables for a parabolic trough collector and depending on whether the heat transfer medium is oil or water, two possible thermodynamic models can be developed as follow:

(a) For a collector system that operates with thermal oil.

The relevant equations used for the development of this model are given in section 3.4.1. The analysis is done on the following assumptions: process is steady-state, the fluid properties are dependent on temperature alone, and the flow in the absorber is a fully developed (hydrodynamically & thermally) turbulent flow in a smooth circular pipe. The input & output variables of the CS Model are shown in Figure 19:

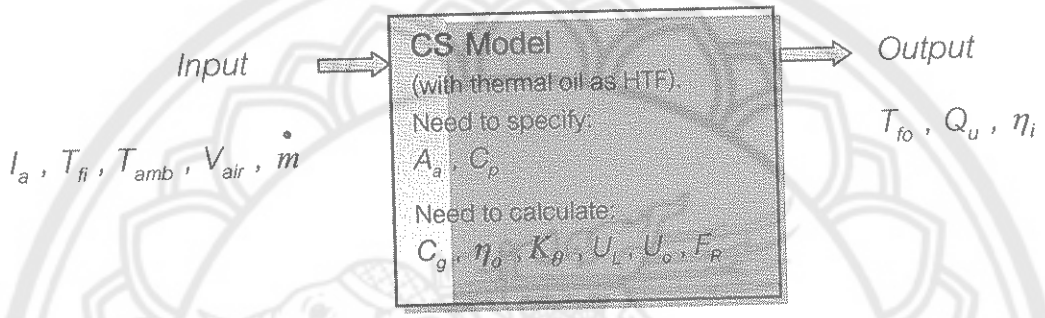

Figure 19 Input & output variables of the CS Model (HTF: oil)

where:

I_a	Direct normal irradiance
A_a	Aperture area
C_g	Geometric concentration ratio
C_p	Specific heat of fluid
V_{air}	Velocity of air
Q_u	Useful gain
T_{amb}	Ambient temperature
T_{fi} , T_{fo}	Collector fluid inlet & outlet temperatures
η_o	Optical efficiency of collector
K_θ	Incidence angle modifier
U_L , U_o	Overall heat loss & heat transfer coefficients
F_R	Collector heat removal factor
$\dot{m}$	Mass flux of fluid
η_i	Collector instantaneous thermal efficiency

(b) For a direct solar steam (DISS) collector system.

In the case of a DISS collector which uses water to produce steam directly in the absorber pipe, the thermodynamic analysis used to create the CS Model is explained in section 3.4.1; and the input & output variables of the model is similar to Figure 19 but with a few additional parameters (Figure 20):

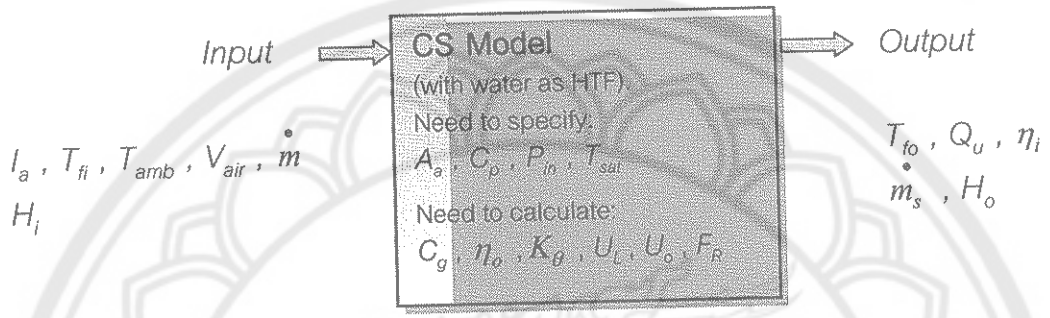

Figure 20 Input & output variables of the CS Model (HTF: water)

where:

P_{in} Process pressure at collector inlet

T_{sat} Saturation temperature of water at P_{in}

H_i , H_o Enthalpies of fluid at collector inlet & outlet

$\dot{m}_s$ Mass flux of steam

3.2.3 Gasifier System (GS) Model

The modeling of the gasifier system is a relatively straightforward process where the useful output energy from the gasifier can be easily determined once the properties and quantity of the input solid fuel are known. The relevant equations used for the development of this model are given in section 3.4.2. The input & output variables of the GS Model are shown in Figure 21:

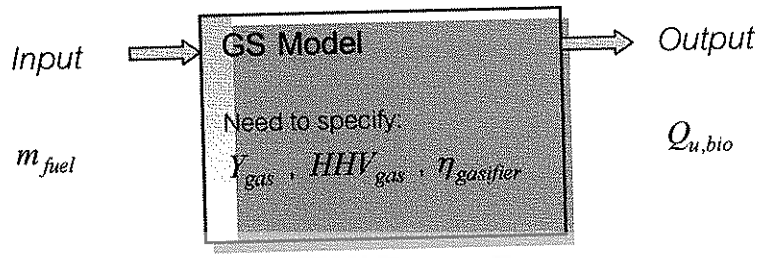

Figure 21 Input & output variables of the GS Model

where:

m_{fuel} Mass of solid biomass fuel

Y_{gas} Yield of gas, in terms of m^3 per kg of solid fuel

HHV_{gas} High heating value of producer gas

$\eta_{gasifier}$ Efficiency of gasifier

$Q_{u,bio}$ Useful energy from gasifier

3.2.4 Thermal Energy Storage (TES) Model

The relevant equations used for the development of this model are given in section 3.4.3. The analysis is done on the basis of a sensible heat storage system with mineral oil as the storage medium. The medium in the storage tank is assumed to be thermally unstratified and fully-mixed. It is also assumed that there are no heat losses between the storage tank and collector so that the temperature of the storage medium is equal to the fluid inlet temperature of the collector. Since a two-tank system is used, thermal discharging is assumed to take place under constant temperature and mass flux conditions. The input & output variables of the TES Model are shown in Figure 22:

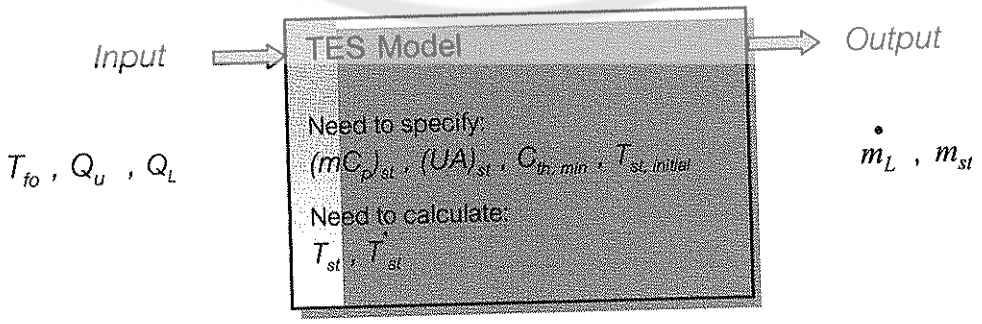

Figure 22 Input & output variables of the TES Model

where:

T_{fo}	Fluid outlet temperature of collector
Q_u	Useful gain of collector
$T_{st,\ initial}$	Initial temperature of storage medium
T_{st}	Temperature of storage medium at the start of each finite time-interval
$\dot{T}_{st}$	Temperature of storage medium at the end of each finite time-interval
Q_L	Energy removal to the PCU [In this study, $Q_L = Q_A$ (section 3.2.5)]
$(mC_p)_{st}$	Mass-specific heat product of the storage medium
$(UA)_{st}$	Loss coefficient – area product of storage tank
$\dot{m}_L$	Mass flux of the load stream
m_{st}	Mass of the storage medium
$C_{th,\ min}$	Minimum thermal storage capacity, in hours

3.2.5 Power Conversion Unit (PCU) Model

The analysis of the steam power cycle is based on the processes that occur in an ideal Rankine cycle. During normal operation, the PCU is assumed to deliver a constant electrical output that is equal to its rated power on an hourly basis. On a typical operation day, it is possible for the PCU to receive heat addition to its boiler from the collector field and gasifier system; while heat addition from the thermal storage tank can take place after normal operation hours to increase the generation capacity of the power plant. A description of the equations used to develop the PCU Model is given in section 3.4.4 while the input and output variables of the model are shown in Figure 23.

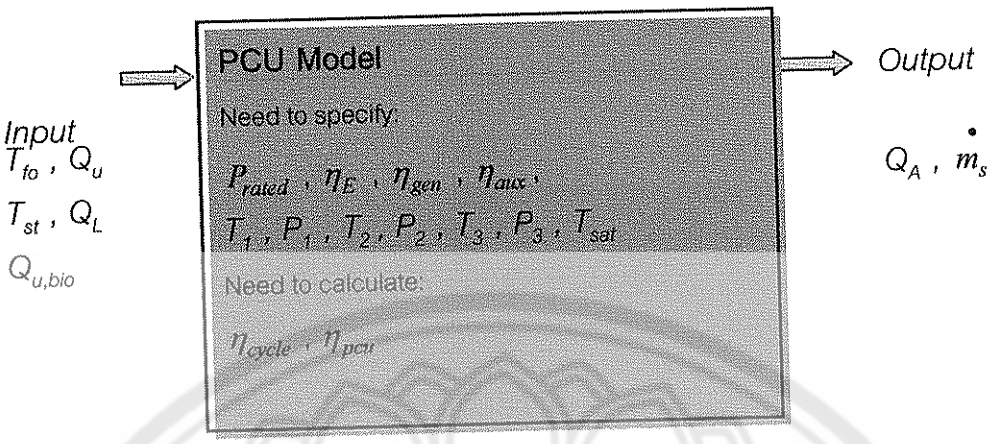

Figure 23 Input & output variables of the PCU Model

where:

P_{rated}	Rated power of the electric generator
η_{cycle}	Thermal efficiency of the Rankine cycle
η_E	Efficiency of expander (engine)
η_{gen}	Efficiency of electric generator
η_{aux}	Efficiency of combustion
η_{pcu}	Efficiency of PCU
Q_A	Energy addition to the boiler of PCU
T_1 , P_1	Temperature & pressure of vapor (steam) at inlet of expander (engine)
T_2 , P_2	Temperature & pressure of mixture at outlet of expander (engine)
T_3 , P_3	Temperature & pressure of fluid (water) at outlet of condenser
T_{sat}	Saturation temperature of water in boiler
$\dot{m}_s$	Mass flux of steam through expander (engine)

3.2.6 Solar Radiation (SR) Model

The SR Model is consisted of two separate sub-routines; one to generate the daily average hourly direct radiation for sunny condition, while the another is used to generate the daily average hourly direct radiation for partly cloudy condition. A detailed description of the method used to formulate this model is given in section 3.3. The input & output variables of the SR Model are shown in Figure 24.

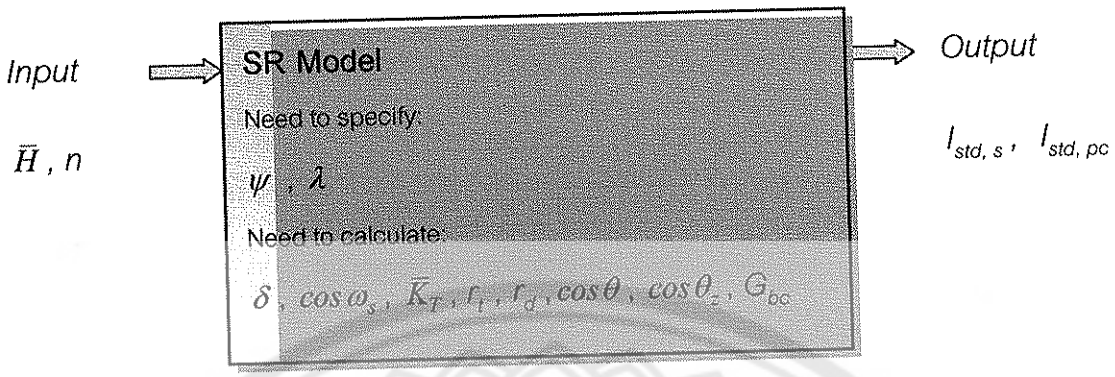

Figure 24 Input & output variables of the SR Model

where:

$\bar{H}$	Monthly average daily global radiation of location (Phitsanulok)
n	Day of the year
ψ	Latitude of location (Phitsanulok)
λ	Altitude of location (Phitsanulok)
δ	Declination angle
$cos\,\omega_s$	Cosine of sunset hour angle
$\bar{K}_T$	Average clearness index
r_t	Ratio of hourly total to daily total global radiation
r_d	Ratio of hourly total to daily total diffuse radiation
$cos\,\theta$	Cosine of the incidence angle
$cos\,\theta_z$	Cosine of the zenith angle
G_{bc}	Clear sky normal beam irradiance on a horizontal surface
$I_{std,\,s}$	Standard average hourly direct radiation of Phitsanulok (Sunny)
$I_{std,\,pc}$	Standard average hourly direct radiation of Phitsanulok (Partly cloudy)

3.3 Solar Radiation (SR) Model of Phitsanulok Province

Duffie & Beckman (1991) have described two methods that are used to estimate direct radiation based on: (a) monthly average daily global radiation (Appendix B), and (b) clear sky radiation (Appendix C) [35]. These methods are used to develop the solar radiation (SR) model for Phitsanulok province. The radiation model is an

auxiliary part of the main BSPP mathematical model and is used to derive the standard curve for the daily average hourly direct radiation of Phitsanulok for both sunny and partly cloudy conditions.

3.3.1 Estimation based on Monthly Average Daily Global Radiation

This method uses the monthly average daily global radiation of a location to estimate the clearness index for that same location. The value of the clearness index is an indication of the probability of cloud cover on a particular site over an extended period of time. Hence, the method presented here is analogous to simulating the solar insolation profile of a location under the condition of partial cloudiness.

(a) Declination.

The declination (δ) is the angular position of the sun at solar noon, with respect to the plane of the equator. Its value in degrees is given by the equation:

$$\delta = 23.45 * \sin\left(360 * \left(\frac{284+n}{365}\right)\right) \quad (3.1)$$

where n is the day of the year (i.e. n = 1 for January 1, n = 32 for February 1, etc.). Table 4 shows the recommended average day of each month and the corresponding value of n (Klein 1977). From equation (3.1), the declination angle varies between -23.45° on December 21 and +23.45° on June 21.

Table 4 Recommended average day of each month & value of n

Month	Jan	Feb	Mar	Apr	May	Jun	Jul	Aug	Sep	Oct	Nov	Dec
Date	17	16	16	15	15	11	17	16	15	15	14	10
Day of Year (n)	17	47	75	105	135	162	198	228	258	288	318	344

(b) Solar hour angle and sunset angle.

The solar hour angle is the angular displacement of the sun east or west of the local meridian; morning negative, afternoon positive. The solar hour angle is equal to

zero at solar noon and varies by 15 degrees per hour from solar noon. For example at 7 am (solar time) the hour angle is equal to -75° (7 am is 5 hours from noon; 5 times 15 is equal to 75, with a negative sign because it is morning). Also, for each hour of the day, the midpoint of the hour is used. Thus, the hour angle for the hour between 1 to 2 pm is equal to 22.5° (1.30 pm is 1.5 hours from noon; 1.5 times 15 is equal to 22.5). The sunset hour angle (ω_s) is the solar hour angle corresponding to the time when the sun sets. It is given by the following equation:

$$\cos \omega_s = -\tan\psi \tan\delta \tag{3.2}$$

where δ is the declination, calculated through equation (3.1), and ψ is the latitude of the site, specified by the user.

(c) Extraterrestrial radiation and clearness index.

Solar radiation outside the earth's atmosphere is called extraterrestrial radiation. Daily extraterrestrial radiation on a horizontal surface (H_o) can be computed for day n from the following equation:

$$H_o = \frac{24*3600G_{sc}}{\pi}\left(1+0.033\cos\left(\frac{360n}{365}\right)\right)\left(\cos\psi\cos\delta\sin\omega_s + \frac{\pi\omega_s}{180}\sin\psi\sin\delta\right) \tag{3.3}$$

where G_{sc} is the solar constant equal to 1,367 W/m^2, and all other variables have the same meaning as before. Before reaching the surface of the earth, radiation from the sun

Table 5 Monthly average daily global radiation on a horizontal surface

Location: Phitsanulok												
Latitude: 16.78°												
Monthly average daily global radiation on a horizontal surface, $\overline{H}$ (MJ/m^2.day)												
Jan	Feb	Mar	Apr	May	Jun	Jul	Aug	Sep	Oct	Nov	Dec	Ave
16.5	18.9	20.6	22.2	19.3	18.1	19.2	18.0	17.8	17.0	17.8	16.7	18.5

is attenuated by the atmosphere and the clouds. The ratio of solar radiation at the surface of the earth to extraterrestrial radiation is called the clearness index. Thus the monthly average clearness index ($\bar{K}_T$) is defined as:

$$\bar{K}_T = \frac{\bar{H}}{\bar{H}_o} \tag{3.4}$$

where $\bar{H}$ is the monthly average daily global radiation on a horizontal surface and $\bar{H}_o$ is the monthly average extraterrestrial daily solar radiation on a horizontal surface. In this study, the $\bar{H}$ values used are shown in Table 5, which can be referenced from [14 &15]. The $\bar{K}_T$ values depend on the location and the time of the year considered; their values are usually between 0.3 and 0.8 (i.e. < 0.3 for very overcast climates and > 0.8 for very sunny locations).

(d) Hourly horizontal global, diffuse and direct (beam) irradiance.

Solar global radiation can be broken down into two components: beam radiation, which emanates from the solar disk, and diffuse radiation, which emanates from the rest of the sky. First, monthly average daily diffuse radiation ($\bar{H}_d$) is calculated from monthly average daily global radiation ($\bar{H}$) using the Erbs et al. (1982) correlation:

$$\frac{\bar{H}_d}{\bar{H}} = 1.391 - 3.560\bar{K}_T + 4.189\bar{K}_T^2 - 2.137\bar{K}_T^3 \tag{3.5}$$

when the sunset hour angle for the average day of the month is less than 81.4°, and:

$$\frac{\bar{H}_d}{\bar{H}} = 1.311 - 3.022\bar{K}_T + 3.427\bar{K}_T^2 - 1.821\bar{K}_T^3 \tag{3.6}$$

when the sunset hour angle is greater than 81.4° (the monthly average clearness index, $\bar{K}_T$ is calculated through equation 3.4). Next, the average daily radiation is broken down into hourly values. This is done with the formulae from Collares-Pereira and Rabl (1979) for global irradiance:

$$r_t = \left(\frac{\pi}{24}\right) * (a + b\cos\omega) * \left(\frac{\cos\omega - \cos\omega_s}{\sin\omega_s - \left(\left(\frac{\pi\omega_s}{180}\right)\cos\omega_s\right)} \right) \tag{3.7}$$

$$a = 0.409 + 0.5016\sin(\omega_s - 60) \tag{3.8}$$

$$b = 0.6609 - 0.4767 \sin(\omega_s - 60) \tag{3.9}$$

where r_t is the ratio of hourly total to daily total global radiation, with ω_s the sunset hour angle, and ω the solar hour angle for the midpoint of the hour for which the calculation is made; and with the formula from Liu and Jordan (1960) for diffuse irradiance:

$$r_d = \left(\frac{\pi}{24}\right) * \left(\frac{\cos\omega - \cos\omega_s}{\sin\omega_s - (\omega_s \cos\omega_s)}\right) \tag{3.10}$$

where r_d is the ratio of hourly total to daily total diffuse radiation. For each hour of the "average day", the global horizontal irradiance (I) and its diffuse and beam components (I_d *and* I_b) are given by:

$$I = r_t \cdot \bar{H} \tag{3.11}$$

$$I_d = r_d \cdot \bar{H}_d \tag{3.12}$$

$$I_b = I - I_d \tag{3.13}$$

(e) Normal beam irradiance on aperture plane of parabolic trough collector.

The direct normal irradiance (DNI) or the beam radiation that incident normally on the aperture plane of a parabolic trough collector (I_a), can be calculated from:

$$I_a = I_b R_b = I_b * \left(\frac{\cos\theta}{\cos\theta_z}\right) \tag{3.14}$$

where I_b is the beam radiation on horizontal surface (calculated through equations 3.11 – 3.13), and R_b is the ratio of beam radiation on a moving collector aperture to that on a horizontal surface. For horizontal surfaces, the angle of incidence is the zenith angle (θ_z) of the sun. Its value must be between 0° and 90° when the sun is above the horizon and is given by:

$$\cos\theta_z = \cos\psi \cos\delta \cos\omega + \sin\psi \sin\delta \tag{3.15}$$

For a parabolic trough collector oriented on a horizontal north-south axis and east-west tracking, the cosine of the incidence angle is:

$$\cos\theta = \left[\left(\cos\psi\cos\delta\cos\omega + \sin\psi\sin\delta\right)^2 + \cos^2\delta\sin^2\omega\right]^{0.5} \quad (3.16)$$

Using the method described above, the monthly average hourly direct radiation of Phitsanulok (under partly cloudy condition), evaluated over a year, is found to be 440 W/m^2 (Figure 25). This result is then used to create the standard curve for daily average hourly direct radiation of Phitsanulok (Figure 26). *From the curve, it is observed that the average hourly direct radiation from 08:00 am to 16:00 pm is approximately 400 W/m^2 and this standard value ($I_{std,\,pc}$) is to be used for all subsequent analysis of the power plant under partly cloudy condition.*

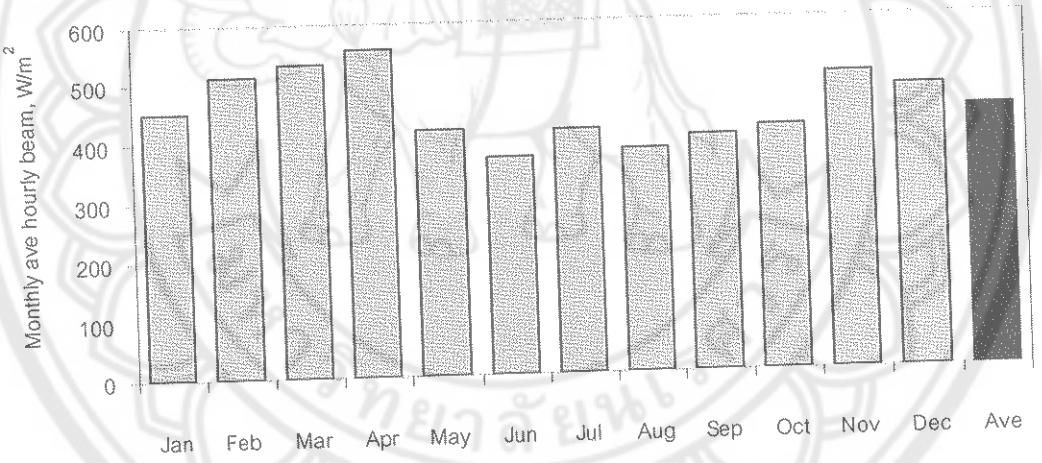

Figure 25 Monthly average hourly direct radiation of Phitsanulok (partly cloudy)

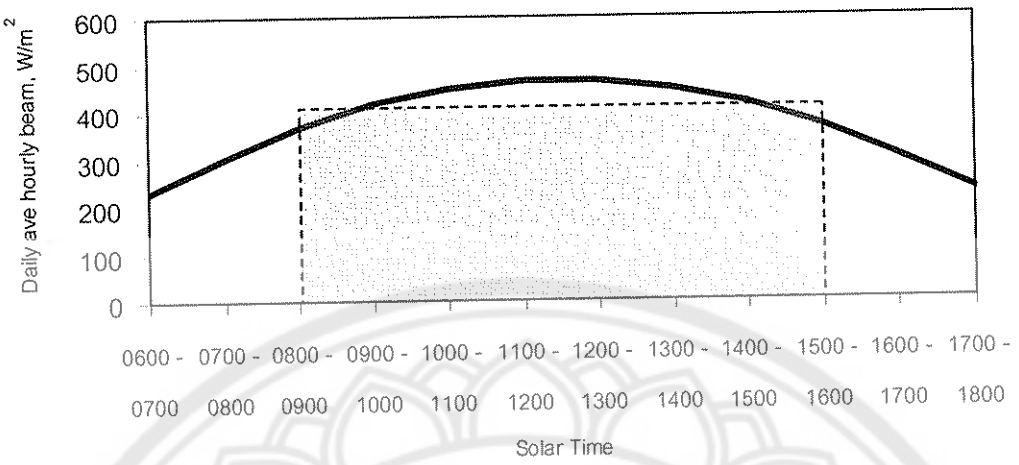

Figure 26 Standard curve for daily average hourly direct radiation of Phitsanulok (partly cloudy)

3.3.2 Estimation based on Clear Sky Radiation

The effects of the atmosphere in scattering and absorbing radiation are variable with time as atmospheric conditions and air mass change. Hence, it is useful to define a standard "clear sky" and calculate the daily and hourly radiation which would be received on an aperture plane under these standard atmospheric conditions. In this section, a method for estimating the beam radiation transmitted through clear atmosphere which takes into account the zenith angle and altitude is presented.

(a) Extraterrestrial radiation.

The method begins with the calculation of the extraterrestrial radiation. The extraterrestrial radiation measured on the plane normal to the radiation (G_{on}) on the nth day of the year, is given by:

$$G_{on} = G_{sc}\left(1+0.033\cos\frac{360n}{365}\right) \tag{3.17}$$

(b)Transmittance for beam radiation.

The atmospheric transmittance for beam radiation (τ_b) is given by the ratio G_{bn}/G_{on} and is expressed in the form:

$$\tau_b = a_o + a_1 exp(-b / cos\theta_z) \quad (3.18)$$

where G_{bn} is the clear sky normal beam irradiance. The constants a_0 , a_1 and b for the standard atmosphere with 23 km visibility are found from, a_0^* , a_1^* and b^*, which are given for altitude less than 2.5 km by:

$$a_0^* = 0.4237 - 0.00821 \ (6.0 - \lambda)^2 \quad (3.19)$$

$$a_1^* = 0.5055 + 0.00595 \ (6.5 - \lambda)^2 \quad (3.20)$$

$$b^* = 0.2711 + 0.01858 \ (2.5 - \lambda)^2 \quad (3.21)$$

where λ is the altitude of the observer in kilometers. Correction factors are applied to a_0^* , a_1^* and b^* to allow for changes in climate types. In the case of tropical climate, the following relations are used: $0.95 = a_0 / a_0^*$, $0.98 = a_1 / a_1^*$, and $1.02 = b / b^*$. Thus, the transmittance of this standard atmosphere for beam radiation can be determined for any zenith angle and any altitude up to 2.5 km.

(c) Hourly clear sky normal beam irradiance on horizontal surface.

The clear sky normal beam irradiance (G_{bn}) is given by:

$$G_{bn} = G_{on}\tau_b \quad (3.22)$$

and the clear sky normal beam irradiance on a horizontal surface (G_{bc}) is:

$$G_{bc} = G_{on}\tau_b \cos\theta_z \quad (3.23)$$

Thus for each hourly period, the clear sky horizontal beam irradiance (I_{bc}) can be expressed as:

$$I_{bc} = G_{bc} = G_{on}\tau_b \cos\theta_z \quad (3.24)$$

(d) Clear sky normal beam irradiance on aperture plane of trough collector.

The clear sky beam irradiance that incident normally on the aperture plane of a parabolic trough collector (I_a) is given by:

$$I_a = I_{bc}R_b = G_{on}\tau_b \cos\theta_z * \left(\frac{\cos\theta}{\cos\theta_z}\right) = G_{on}\tau_b \cos\theta \qquad (3.25)$$

Using the method described above, the monthly average hourly direct radiation of Phitsanulok (under sunny condition), evaluated over a year, is found to be 749 W/m^2 (Figure 27). This result is then used to create the standard curve for daily average hourly direct radiation of Phitsanulok (Figure 28). *From the curve, it is observed that the average hourly direct radiation from 08:00 am to 16:00 pm is approximately 700 W/m^2 and this standard value ($I_{std,s}$) is to be used for all subsequent analysis of the power plant under sunny condition.*

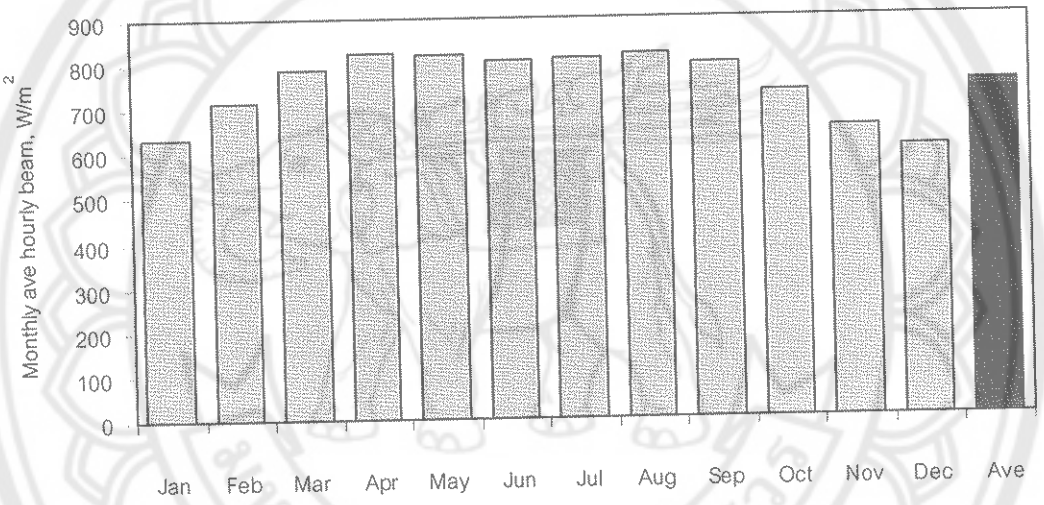

Figure 27 Monthly average hourly direct radiation of Phitsanulok (sunny)

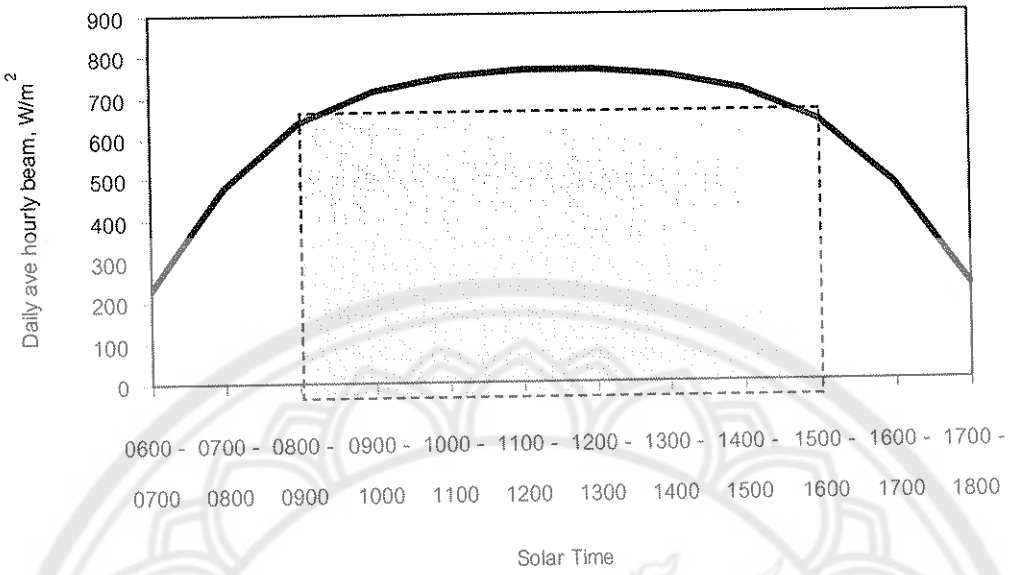

Figure 28 Standard curve for daily average hourly direct radiation of Phitsanulok (sunny)

3.4 Thermodynamic Analysis and Calculation

The following section presents the algorithm and the mass & energy balance equations used to develop the mathematical models for the collector system, gasifier system, thermal energy storage unit & power conversion unit, which together make up the entire model of the proposed power plant. The associated flow diagrams are given in Appendices D, F, G, E & H respectively.

3.4.1 Analysis of the Collector System

The standard procedure for solar collector performance testing and analysis has been well documented in ASHRAE (1977) [36]. The process for thermal analysis of a solar trough collector is generally similar to that of a flat-plate collector. In general, the instantaneous useful energy gain of a trough collector in terms of the absorber wall temperature T_r operating under steady conditions can be expressed as

$$Q_u = A_a I_a \left(\eta_o K_\theta\right) - A_r U_L \left(T_r - T_{amb}\right) \tag{3.26}$$

where A_a is the collector aperture area, A_r is the absorber surface area, I_a is the solar irradiation, η_o is the collector optical efficiency, K_θ is the incidence angle modifier, U_L is

the collector heat loss coefficient, and T_{amb} is the ambient temperature. Using equation (3.26) and dividing both sides by $A_a I_a$, the instantaneous thermal efficiency of a trough collector with concentration ratio C_g is given by

$$\eta_i = \frac{Q_u}{A_a I_a} \tag{3.27}$$

$$= (\eta_o K_\theta) - \frac{U_L}{C_g} \cdot \frac{(T_r - T_{amb})}{I_a} \tag{3.27a}$$

In this study, the effective A_a is used in all calculations. The effective A_a is derived from the effective W which is aperture width W minus the outside diameter D_o of the absorber pipe. Performing an overall energy balance on the fluid in the collector in terms of the fluid outlet (exit) temperature T_{fo} and fluid inlet temperature T_{fi} will yield

$$Q_u = \dot{m} C_p (T_{fo} - T_{fi}) \tag{3.28}$$

where $\dot{m}$ is the mass flux and C_p is the fluid specific heat. In the case of a trough collector generating direct solar steam (DISS)

$$Q_u = \dot{m}(H_o - H_i) \tag{3.29}$$

where H_o and H_i are the specific enthalpies at the exit and entry points of the DISS collector respectively.

Apart from the instantaneous performance, it is also useful to know how a collector would behave under varying solar radiation conditions over the long term. The algorithm of the collector model begins with a simple overall energy balance relationship where the thermal output of the collector is dependent on the heat absorbed reduced by the heat losses of the collector, such that

$$Q_u = Q_{abs} - Q_{loss} \tag{3.30}$$

Based on the classical Hottel-Whillier-Bliss equation which relates Q_u to the fluid inlet temperature T_{fi} and ambient temperature T_{amb} , equation (3.26) can be expressed in a more convenient form as

$$Q_u = A_a F_R S - \frac{A_a F_R U_L}{C_g}\left(T_{fi} - T_{amb}\right) \tag{3.31}$$

The absorbed heat Q_{abs} can be estimated from the absorbed radiation per unit aperture area S and the collector heat removal factor F_R; while the thermal losses Q_{loss} can be evaluated from F_R , the collector heat loss coefficient U_L and the concentration ratio C_g.

(a) Collector absorbed heat.

The first part of the thermodynamic analysis is concerned with the estimation of the absorbed heat. The quantity of absorbed heat varies with the aperture area A_a, F_R, solar irradiation I_a, optical efficiency η_o , and the incidence angle modifier K_θ , where

$$\begin{aligned} Q_{abs} &= A_a \cdot F_R \cdot I_a \cdot \eta_o \cdot K_\theta \\ &= A_a \cdot F_R \cdot S \end{aligned} \tag{3.32}$$

The solar irradiation I_a is the normal beam radiation projected on the aperture, corrected for the "cosine effect" due to the angular deviation of the sun beam from the normal of the aperture plane, so that

$$I_a = I_{bn} \cdot \cos\theta \tag{3.33}$$

where I_{bn} is the direct normal irradiation and θ is the incidence angle. For a parabolic trough collector oriented on a horizontal north-south axis

$$\cos\theta = \left(\cos^2\theta_z + \cos^2\delta \sin^2\omega\right)^{0.5} \tag{3.34}$$

and

$$\cos\theta_z = \cos\phi\cos\delta\cos\omega + \sin\phi\sin\delta \tag{3.35}$$

The optical efficiency η_o of an imaging concentrator, such as the parabolic trough collector, depends on the material and geometry of the device and is an indication of how well the collector has been designed and fabricated. It is defined as a ratio of the

absorbed radiation by the receiver to the beam radiation projected on the aperture. It can be expressed in terms of the specular reflectance ρ of the concentrator, transmittance-absorptance product $(\tau\alpha)$ of the receiver and the intercept factor γ, so that

$$\eta_o = \rho \cdot (\tau\alpha) \cdot \gamma \tag{3.36}$$

The intercept factor is defined as the fraction of reflected radiation that is incident on the absorbing surface of the receiver. Its value is dependent on the receiver geometry and imaging errors due to surface distortion and misalignment. Kalogirou (1995) [37] has presented a simplified method for estimating the intercept factor of parabolic trough collectors based on the "universal error parameters" correlation of Guven and Bannerot (1985) [38]. Using the universal error parameters, the formulation of the intercept factor γ can be expressed as

$$\gamma = \frac{1+\cos\phi_{rim}}{2\sin\phi_{rim}} \int_0^{\phi_{rim}} \left[\frac{\sin\phi_{rim}\left(1+\cos\phi_{rim}\right)\left(1-2d^*\sin\phi_{rim}\right)-\pi\beta^*\left(1+\cos\phi_{rim}\right)}{\sqrt{2}\pi\sigma^*\left(1+\cos\phi_{rim}\right)} \right]$$
$$-\left[-\frac{\sin\phi_{rim}\left(1+\cos\phi_{rim}\right)\left(1+2d^*\sin\phi_{rim}\right)+\pi\beta^*\left(1+\cos\phi_{rim}\right)}{\sqrt{2}\pi\sigma^*\left(1+\cos\phi_{rim}\right)} \right] \frac{d\phi_{rim}}{\left(1+\cos\phi_{rim}\right)} \tag{3.37}$$

where:

ϕ_{rim} Rim angle (degree)

σ^* Universal random error parameter

β^* Universal nonrandom error parameter due to angular errors

d^* Universal nonrandom error parameter due to receiver & reflector errors

According to the study by Kalogirou (1995), the value of the intercept factor for a carefully fabricated parabolic trough collector was found to be γ = 0.9506. However in this instance, the necessary laboratory setup to measure the universal random & nonrandom error parameters is not available. Hence for the purpose of this study, the intercept factor is assumed to be 0.89 (Table 1), based on the value of the LS-2 collector, since the LS-2 & EPC collectors share similar dimensions and geometry.

The incidence angle modifier K_θ is a parameter that groups all the non-normal incident effects that cause reflected rays to be scattered or to miss the receiver into a convenient factor. Its value can be represented by a polynomial function in the form:

$$K_\theta = 1 - a_1\theta - a_2\theta^2 - a_3\theta^3 - a_4\theta^4 \tag{3.38}$$

where a_1 to a_4 are empirical constants. Quaschning (2001) [39] reported the incidence angle modifier for the LS-2 collector as: $K_\theta = 1 - 8.84\text{x}10^{-4}\ \theta - 5.369\text{x}10^{-5}\ \theta^2$, which is the value used in this study since the LS-2 & EPC collectors share similar dimensions and geometry.

(b) Collector heat losses.

The next part of the thermodynamic analysis is concerned with the estimation of the collector's thermal losses. From equation (3.31), the expression for thermal losses is given by

$$Q_{loss} = \frac{A_a F_R U_L}{C_g}\left(T_{fi} - T_{amb}\right) \tag{3.39}$$

The thermal energy of a parabolic trough collector can be assumed to be lost in the following manner:

(i) Heat loss by radiation and convection from the absorber wall to the glass cover, defined by the respective heat transfer coefficients $h_{rad,\ r\text{-}c}$ and $h_{conv,\ r\text{-}c}$.

(ii) Heat loss from the glass cover by radiation to the sky and by convection to the ambient, defined by the respective heat transfer coefficients $h_{rad,\ c\text{-}a}$ and h_{wind}.

(iii) Heat loss by conduction through the support structure and end bellows. However in this instance, only the radiation and convection factors are considered since they account for the bulk of the collector's total losses. The respective radiation and convection coefficients are then evaluated using the appropriate equations given in references [35, 40 & 41] and combined into a single factor known as the overall heat loss coefficient U_L, such that:

$$U_L = \left[\frac{A_r}{\left(h_{wind} + h_{rad,c-a}\right) A_c} + \frac{1}{\left(h_{conv,r-c} + h_{rad,r-c}\right)} \right]^{-1} \tag{3.40}$$

$$h_{wind} = \frac{Nu \cdot k_{air}}{D_c} \tag{3.41}$$

use $N_u = 0.40 + 0.54\, Re_{air}^{0.52}$ for $0.1 < Re_{air} < 1000$ (3.41a)

or $N_u = 0.3\, Re_{air}^{0.6}$ for $1000 < Re_{air} < 50000$ (3.41b)

$$Re_{air} = \frac{\rho_{air} \cdot V_{air} \cdot D_c}{\mu_{air}} \tag{3.41c}$$

$$h_{rad,c-a} = \left(5.67x10^{-8}\right) \varepsilon_c 4 T_{av,c-a}^3 \tag{3.42}$$

$$h_{conv,r-c} = \frac{N_u \cdot k_{air}}{0.5\left(D_c - D_r\right)} \tag{3.43}$$

use $$N_u = 0.317\left(10^6\right)^{0.25} \left[\left(\frac{D_c - D_r}{2} \right)^3 \left(\frac{1}{D_r^{0.6}} + \frac{1}{D_c^{0.6}} \right)^5 \right]^{-0.25} \tag{3.43a}$$

$$h_{rad,r-c} = \frac{\left(5.67x10^{-8}\right) \cdot \left(T_r^2 + T_c^2\right) \cdot \left(T_r + T_c\right)}{\frac{1-\varepsilon_r}{\varepsilon_r} + 1 + \frac{\left(1-\varepsilon_c\right) D_r}{\varepsilon_c D_c}} \tag{3.44}$$

where:

A_r Surface area of absorber

A_c Surface area of glass cover

N_u Nusselt number

R_e Reynolds number

k_{air} Thermal conductivity of air

ρ_{air} Density of air

V_{air} Velocity of air

μ_{air} Kinematic viscosity of air

D_r Diameter of absorber

D_c Diameter of glass cover

ε_r Emittance of absorber

ε_c Emittance of glass cover

T_r Temperature of absorber

T_c Temperature of glass cover

To account for the heat transfer from the surroundings to the fluid in the absorber, a parameter known as the overall heat transfer coefficient U_o is defined, such that

$$U_o = \left[\frac{1}{U_L} + \frac{D_o}{h_f D_i} + \frac{D_o In(D_o / D_i)}{2k} \right]^{-1} \tag{3.45}$$

where D_i and D_o are the absorber inside and outside diameters, h_f is the heat transfer coefficient inside the absorber, and k is the thermal conductivity of the absorber pipe. For fully developed turbulent flow inside a pipe, the Petukhov equation [35] can be used:

$$Nu = \frac{(f/8)\,Re\,Pr}{1.07 + 12.7\sqrt{f/8}\left(Pr^{2/3} - 1\right)} \left(\frac{\mu}{\mu_w} \right)^n \qquad \text{for Re > 2200} \tag{3.46}$$

$$Nu = 3.7 \qquad \text{for Re < 2200} \tag{3.47}$$

$$Re = \frac{4 \cdot \dot{m}}{\pi \cdot D_i \cdot \mu} \tag{3.48}$$

where n = 0.11 for heating and 0.25 for cooling and the Darcy friction factor f for smooth pipes is given by

$$f = \left(0.79 \ln Re - 1.64\right)^{-2} \tag{3.49}$$

$$h_f = \frac{Nu \cdot k}{D_i} \tag{3.50}$$

where:

Pr Prandlt number of fluid

μ Kinematic viscosity of fluid

μ_w Kinematic viscosity of water

$\dot{m}$ Mass flux of fluid

n 0.11

The collector efficiency factor F' which represents the ratio of the actual useful energy gain to the useful gain that would result if the absorber surface had been at the local fluid temperature can now be expressed as

$$F' = \frac{U_o}{U_L} = \frac{1/U_L}{\frac{1}{U_L} + \frac{D_o}{h_f D_i} + \left(\frac{D_o}{2k} In \frac{D_o}{D_i}\right)} \tag{3.51}$$

However, it is convenient to define a heat removal factor F_R that relates the actual useful energy gain of a collector to the useful gain if the entire absorber surface were at the fluid inlet temperature. Thus, from equations (3.28) and (3.31), F_R can be expressed as

$$F_R = \frac{\dot{m} C_p \left(T_{fo} - T_{fi}\right)}{A_a \left[I_a \eta_o K_\theta - \frac{U_L}{C_g}\left(T_{fi} - T_{amb}\right)\right]} \tag{3.52}$$

Alternatively, F_R is also a measure of the collector performance as a heat exchanger since it is the ratio of the actual heat transfer to the maximum possible heat transfer and

is related to F' by

$$\frac{F_R}{F'} = \frac{\dot{m}C_p}{A_r U_L F'}\left[1 - exp\left(-\frac{A_r U_L F'}{\dot{m}C_p}\right)\right] \tag{3.53}$$

Hence, once the values of F_R and U_L are known, they are substituted into equations (3.39), (3.32), (3.30) and (3.28), whereby the useful energy gain of the collector and the corresponding fluid outlet temperature can be evaluated.

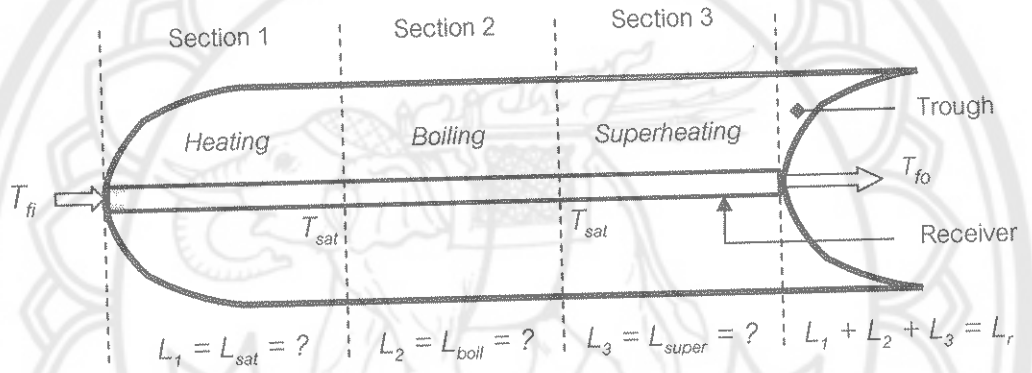

Figure 29 Evaluation sections of a DISS collector

(c) Special case of Direct Solar Steam (DISS).

However, in the case of a DISS collector where a part of the receiver serves as a boiler and other parts as fluid heaters, the different sections of the receiver will have to be considered separately. The analysis begins with the assumption that the receiver is consisted of three possible sections with length L_1 , L_2 & L_3 , corresponding to the heating, boiling & superheating portions of the collector respectively (Figure 29).

L_{sat} , L_{boil} , L_{super} & L_r refer to the length to heat water to saturation temperature (T_{sat}) , length to boil for complete vaporization, length to superheat steam, & length of receiver respectively. In this instance, equation (3.31) is not used to evaluate the useful gain of the collector since the length of the trough to heat the fluid temperature to the saturation temperature is not known. Instead, equation (3.54) is used which calculates the useful gain per meter based on the fluid temperature:

$$q_u' = F' \frac{A_a}{L}\left[S - \frac{A_r}{A_a} U_L \left(T_f - T_{amb} \right) \right] \quad (3.54)$$

where:

T_f = $[(T_{in} + T_{sat}) / 2]$

T_{in} = Temperature of water into the trough

T_{sat} = Saturation temperature of water at P_{in}

P_{in} = Pressure at collector inlet

Next, evaluating for section 1 (refer to Figure 29) and using equation (3.55), the length to heat the water to saturation (L_{sat}) is calculated by:

$$L_{sat} = \left(T_{sat} - T_{in} \right) \frac{C_p \cdot m_w}{q_u'} \quad (3.55)$$

where C_p is the specific heat of water and m_w is the mass of water. If length L_{sat} is calculated to be > L_r , then let $L = L_r$ and the useful gain can be evaluated in the usual manner using equation (3.31). If L_{sat} is < L_r , then the analysis will proceed to evaluating for section 2 and calculate length L_{boil} using equation (3.56):

$$L_{boil} = \frac{H_{fg} \cdot m_w}{q_u'} \quad (3.56)$$

where H_{fg} is the heat of vaporization of water. The quality of the steam (x) can then be calculated by equation (3.57) and the mass of steam m_s can be found by equation (3.58).

$$x = \frac{L_r - L_{sat}}{L_{boil}} \quad (3.57)$$

$$m_s = x \cdot m_w \quad (3.58)$$

If the length to saturation L_{sat} is greater than or equal to the length of the receiver L_r , then the quality of steam is zero and the mass of steam out of the trough is zero. If steam is produced, the specific enthalpy of the steam leaving the trough without being superheated can be calculated by:

$$H_o = H_f + \left(x \cdot H_{fg}\right) \tag{3.59}$$

where H_f is the specific enthalpy of water at the saturation temperature. Continuing to the 3rd section of the analysis, if length L_{boil} is > L_r , the steam leaves the trough as saturated steam without superheating. On the other hand, if L_{boil} is < L_r , then $L_{super} = L_r - L_{boil}$ and evaluation of the useful gain can proceed in the usual manner since the length is known. In this instance, the properties of fluid used in the analysis are those of superheated steam.

3.4.2 Analysis of the Gasifier System

Compared to the parabolic trough collector, the analysis needed to develop the model for the gasifier system is relatively less complicated. This is because, unlike in the collector system where the input solar energy changes with time & is uncontrollable, the energy conversion process in the gasifier system follows a more predictable path, where the amount of input fuel can be controlled and converted into useful energy based on known conversion factors. Irrespective of the design and type of gasifier system, the general equation for the conversion of solid biomass fuel into a combustible gas mixture that is burned to produce useful energy, can be expressed as:

$$Q_{u,bio} = m_{fuel} \cdot Y_{gas} \cdot HHV_{gas} \cdot \eta_{gasifier} \tag{3.60}$$

where:

m_{fuel} Mass of solid biomass fuel

Y_{gas} Yield of gas, in terms of m^3 per kg of solid fuel

HHV_{gas} High heating value of producer gas

$\eta_{gasifier}$ Efficiency of gasifier

In this study, the main purpose of the gas storage tank is to serve as a buffer to compensate for the supply delay during the startup of the gasifier (Figure 17). If the gasifier requires a maximum of 15 minutes for a cold start, there must be a minimum volume of gas in the storage tank that can be supplied to the boiler to enable electricity

generation at the rated power for 15 minutes. The minimum gas volume that must be maintained in the storage tank can be evaluated by the following equation:

$$Vol_{gas} = \frac{P_{rated} \cdot (3.6) \cdot t \cdot Y_{gas}}{\eta_{pcu} \cdot \eta_{aux} \cdot HHV_{gas}} \quad (3.61)$$

where:

P_{rated} Rated power of electric generator, in kW

t Operation time of PCU, in hours

η_{pcu} Efficiency of PCU

η_{aux} Efficiency of combustion

Applying equation (3.61) to the proposed BSPP on the basis of the following conditions where: P_{rated} = 20 kW_e , t = 0.25 , η_{pcu} = 0.2343 (from section 3.4.4), η_{aux} = 0.75 (assumed), HHV_{gas} of producer gas from rice husk = 11.11 MJ/kg and Y_{gas} = 1.60 m^3/kg [26], the minimum volume of gas in the storage tank is estimated to be

$$Vol_{gas} = \frac{(20) \cdot (3.6) \cdot (0.25) \cdot (1.60)}{(0.2343) \cdot (0.75) \cdot (11.11)}$$

$$= 14.75 \ \ m^3$$

Referring to Figure 14 and taking an overall energy balance on the proposed power plant, the general energy equation of the power plant when it is operating in the "hybrid" mode, can be expressed as:

$$Q_u + (Q_{u,bio} \cdot \eta_{aux}) = \frac{P_{rated} \cdot (3.6) \cdot t}{\eta_{pcu}} \quad (3.62)$$

where:

Q_u Useful gain from collector system

$Q_{u,bio}$ Useful energy from gasifier system

3.4.3 Analysis of the Thermal Energy Storage System

In view of its reliability, the preferred method for thermal energy storage in this study is to use sensible heat storage with mineral oil as the storage media. When considering the energy balance on the storage unit, a conservative approach is adopted by assuming that the hot liquid in the tank is well-mixed and the liquid temperature is always uniform for a given time interval. A schematic of such a thermal energy storage (TES) system is shown in Figure 30.

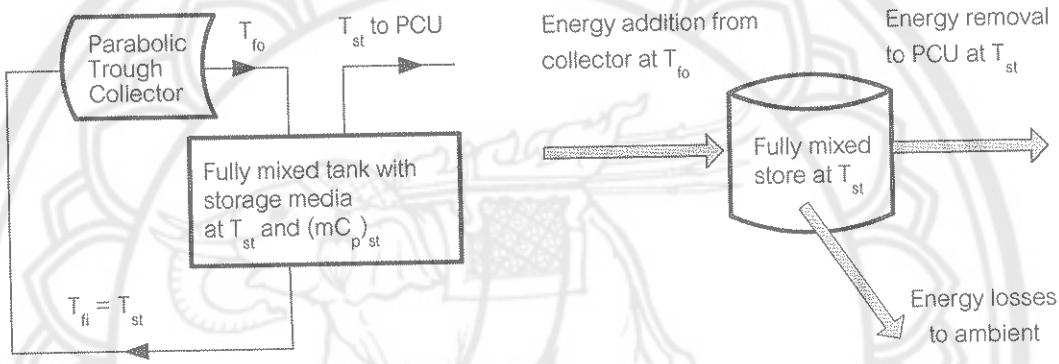

Figure 30 Sensible heat storage with thermal oil

From references [35, 40 & 42], the following equations for a well-mixed liquid, sensible heat storage system, are obtained. The energy storage capacity of a liquid storage unit at uniform temperature (i.e. fully mixed or unstratified) operating over a finite temperature difference is given by:

$$Q_{st} = \left(mC_p\right)_{st} \Delta T_{st} \tag{3.63}$$

where Q_{st} is the total heat capacity for a cycle operating through the temperature range ΔT_{st} , and $\left(mC_p\right)_{st}$ is the mass-specific heat product of the storage medium. For a non-stratified tank, as shown in Figure 30, an energy balance on the tank yields:

$$\left(mC_p\right)_{st} \frac{dT_{st}}{dt} = Q_u - Q_L - \left(UA\right)_{st}\left(T_{st} - T_{amb}\right) \tag{3.64}$$

where Q_u and Q_L are rates of energy addition from the collector and energy removal to the PCU (load), UA is the heat transfer coefficient – area product of the storage tank, T_{st} is the temperature of storage medium, and T_a is the ambient temperature. Equation (3.64) is to be integrated over time to determine the long-term performance of the storage unit and the solar process. There are several possible integration methods, but Duffie & Beckman (1991) [35] suggested using simple Euler integration (i.e. rewriting in finite difference form and solving for the tank temperature at the end of a time increment). Hence for a finite time interval Δt, where the amount of heat addition and removal is assumed to be constant, equation (3.64) can be written for each time interval as:

$$T_{st}^{*} = T_{st} + \frac{\Delta t}{\left(mC_p\right)_{st}}\left[Q_u - Q_L - \left(UA\right)_{st}\left(T_{st} - T_{amb}\right)\right] \tag{3.65}$$

whereby the temperature at the end of an hour is calculated from that at the beginning, assuming that temperatures do not change during the hour. The terms Q_u and Q_L in equation (3.64) are rates; whereas in equation (3.65) they are integrated quantities for the hour. In the case where the liquid flows directly into and out of storage, and assuming no temperature drop between storage tank and collector, i.e. the temperature of liquid leaving the storage tank (T_{st}) is equal to that entering the collector (T_{fi}), then the rate of heat addition to storage tank during the *charging phase* is given by:

$$Q_u = \left(\dot{m}C_p\right)_c \left(T_{fo} - T_{st}\right) \tag{3.66}$$

where $\left(\dot{m}C_p\right)_c$ is the product of the specific heat and mass flux of fluid through the collector. Similarly, the rate of heat withdrawal by the load (Q_L) during the *discharging phase* can be expressed as:

$$Q_L = \left(\dot{m}C_p\right)_L \left(T_{st,act} - T_{bo}\right) \tag{3.67}$$

where $\left(\dot{m}C_p\right)_L$ is the product of the specific heat and load stream mass flux through the steam boiler, $T_{st,\,act}$ is the actual storage temperature, and T_{bo} is the fluid (oil) outlet temperature at the exit of the boiler.

By applying equations (3.65) to (3.67), the charging and discharging processes of the TES unit can be evaluated. In this study, an example of such an analysis is done based on the following assumptions: (a) The useful gain Q_u is derived from a collector similar in design to the EPC, (b) The heat withdrawal by the load Q_L is equal to the heat addition to the boiler Q_A at rated power, (c) The storage medium is Therminol XP, (d) The initial storage temperature $T_{st,\,initial}$ is assumed to be 100 °C at the start of the charging phase, (e) The desired storage temperature $T_{st,\,des}$ is set at 250 °C, (f) The saturation temperature in the steam boiler is set at 165 °C, and (g) The desired minimum storage capacity $C_{th,\,min}$ is set at six hours.

Table 6 shows the evaluation of the charging and discharging processes of the TES unit in the case of sunny weather condition. It is observed that when the collector fluid outlet temperature attains 271 °C in eight hours of operation from 08:00 am to 16:00 pm, the corresponding storage medium temperature can reach 255 °C. During the discharging phase, the storage medium is assumed to exit the tank at a constant temperature. This is possible if the storage tank is assumed to be un-stratified, well-fabricated & well-insulated, and the *UA* parameter is very small compared to the total heat capacity of oil in the storage tank. When discharging at the actual storage temperature $T_{st,\,act}$ of 255 °C, the load stream mass flux $\dot{m}_L$ that is required to sustain electricity generation at rated power is calculated to be 1,027 kg/hr (0.285 kg/s). Applying this hourly mass flux, the total mass of the load stream m_L that is needed for a $C_{th,\,min}$ of six hours is determined to be 6,163 kg. *For practical reason, this value is rounded up to 7,000 kg and this is the mass of storage medium* m_{st} *that can be charged during sunny condition to provide another 6.8 hours of electricity generation at rated power.*

Table 6 Charging and discharging processes of thermal energy storage (sunny)

Charging Phase				*Discharging Phase*				
Time of charge	T_{fo} (°C)	T_{st} (°C)	T^{*}_{st} (°C)	Hour of discharge	Desired storage temp $T_{st,\,des}$ (°C)	Actual storage temp $T_{st,\,act}$ (°C)	$\dot{m}_L$ (kg/hr)	$\sum m_L$ (kg)
08:00-09:00	137	100	119	1st	250	255	1027	1027
09:00-10:00	160	119	140	2nd	250	255	1027	2054
10:00-11:00	181	140	161	3rd	250	255	1027	3081
11:00-12:00	202	161	182	4th	250	255	1027	4108
12:00-13:00	222	182	202	5th	250	255	1027	5136
13:00-14:00	240	202	222	6th	250	255	1027	6163
14:00-15:00	257	222	240	7th	250	255	1027	7190
15:00-16:00	271	240	255	8th	250	255	1027	8217

Table 7 Charging and discharging processes of thermal energy storage (partly cloudy)

Charging Phase				*Discharging Phase*				
Time of charge	T_{fo} (°C)	T_{st} (°C)	T^{*}_{st} (°C)	Hour of discharge	Desired storage temp $T_{st,,\,des}$ (°C)	Actual storage temp $T_{st,\,act}$ °C)	$\dot{m}_L$ (kg/hr)	$\sum m_L$ (kg)
08:00-09:00	121	100	111	1st	250	194	1135	1135
09:00-10:00	135	111	123	2nd	250	194	1135	2270
10:00-11:00	148	123	136	3rd	250	194	1135	3404
11:00-12:00	161	136	149	4th	250	194	1135	4539
12:00-13:00	174	149	161	5th	250	194	1135	5674
13:00-14:00	185	161	173	6th	250	194	1135	6809
14:00-15:00	195	173	184	7th	250	194	1135	7943
15:00-16:00	203	184	194	8th	250	194	1135	9078

Table 7 is similar to Table 6 but in the case of partly cloudy condition. The main difference is that due to the lower radiation available, the temperature of the storage medium can only reach a maximum of 194 °C after eight hours of charging. Hence

during the discharging phase, the actual discharge temperature is 194 °C. This means that a higher $\dot{m}_L$ of 1,135 kg/hr (0.315 kg/s) and a total m_L of 6809 kg is required to maintain a $C_{th,\,min}$ of six hours. *For a m_{st} of 7,000 kg that is charged during partly cloudy condition, it is possible to provide another 6.2 hours of electricity generation at rated power.*

3.4.4 Analysis of the Power Conversion Unit

In an actual power plant, the design of the power conversion unit (PCU) or power block can be rather complicated, involving a series of preheating & reheating and other processes in order to increase the performance & thermal efficiency of the power cycle. However in this study, the power cycle is analyzed in terms of an ideal Rankine cycle in order to highlight the principal processes of a basic steam thermal cycle.

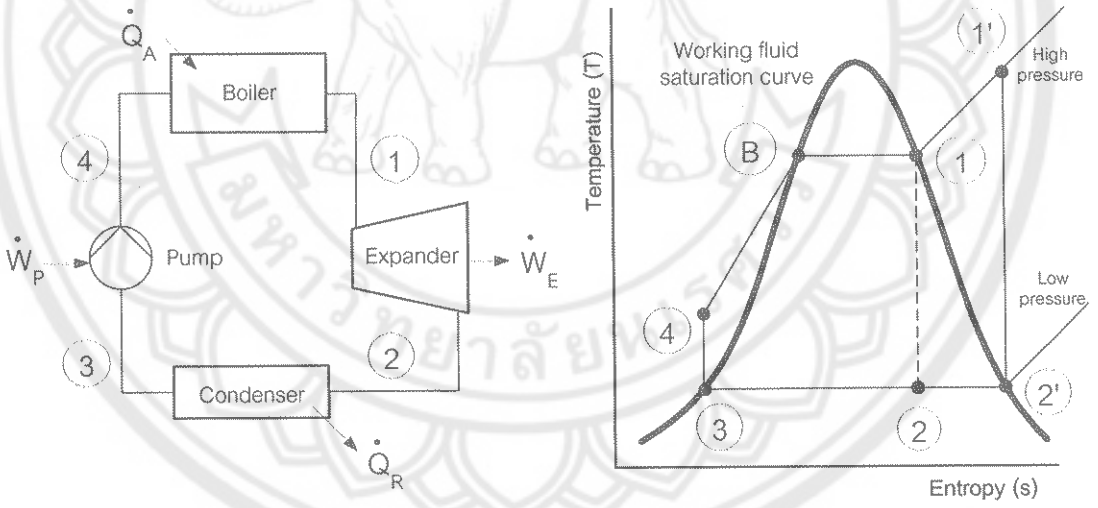

Figure 31 Flow diagram and T-S diagram of a Rankine cycle

The basic components of a Rankine cycle are shown in Figure 31 along with the thermodynamic states of the working fluid. The processes of the reversible cycle are:

(a) 1 – 2 or 1' – 2' Adiabatic reversible expansion through the expander. The exhaust vapor at 2 or 2' is usually in the two-phase region.

(b) 2 – 3 or 2' – 3 Constant temperature and, being a two-phase mixture process, constant-pressure heat rejection ($\dot{Q}_R$) in the condenser.

(c) 3 – 4 Adiabatic reversible compression by the pump of saturated liquid at the condenser pressure, 3, to subcooled liquid at the boiler pressure, 4.

(d) 4 – 1 or 4 – 1' Constant-pressure heat addition ($\dot{Q}_A$) in the boiler. Line 4-B-1-1' is a constant-pressure line.

The Rankine cycle as shown is internally reversible so that the expander and pump are adiabatic reversible and hence vertical on the T-S diagram; no pressure losses occur in the piping so that line 4-B-1-1' is a constant-pressure line. The thermodynamic analysis of the processes in the cycle on a unit time-interval basis is as follow [34]:

Heat addition $$\dot{Q}_A = \dot{m}(H_1 - H_4) = \frac{P_{rated} \cdot (3.6) \cdot t}{\eta_{pcu}} \quad (3.68)$$

Expander work $$\dot{W}_E = \dot{m}(H_1 - H_2) = \frac{\dot{Q}_E}{\eta_E} \quad (3.69)$$

Heat removal $$\left|\dot{Q}_R\right| = \dot{m}(H_2 - H_3) \quad (3.70)$$

Pump work $$\left|\dot{W}_p\right| = \dot{m}(H_4 - H_3) \quad (3.71)$$

Net work $$\Delta\dot{W}_{net} = \dot{m}\left[(H_1 - H_2) - (H_4 - H_3)\right] \quad (3.72)$$

Thermal efficiency $$\eta_{cycle} = \frac{\Delta\dot{W}_{net}}{\dot{Q}_A} = \frac{(H_1 - H_2) - (H_4 - H_3)}{(H_1 - H_4)} \quad (3.73)$$

$$\cong \frac{H_1 - H_2}{H_1 - H_3} \quad (3.73a)$$

where:

P_{rated}	Rated power of electric generator, in kW
t	Operation time of PCU, t = 1 hour
η_{pcu}	Efficiency of PCU
$\dot{Q}_E$	Mechanical energy from expander to electric generator
$\dot{m}$	Hourly mass flux of fluid (or vapor)
H_1, H_2, H_3, H_4	Specific enthalpies of working fluid at positions 1 - 4 of Rankine cycle

For small units where the difference between P_4 & P_3 is not too large and $H_4 \cong H_3$ such that the pump work is negligible compared with the expander work, then the thermal efficiency of the Rankine cycle η_{cycle} may be simplified with little error to $(H_1 - H_2)/(H_1 - H_3)$ [34]. Hence, the overall efficiency of the power conversion unit η_{pcu} can be calculated by:

$$\eta_{pcu} = \eta_{cycle} \cdot \eta_E \cdot \eta_{gen} \tag{3.74}$$

where η_E and η_{gen} are the efficiencies of the expander (engine) and electric generator respectively.

In this study, the thermodynamic states (define by temperature T and pressure P) of the working fluid at positions 1 to 3 of the Rankine cycle in the proposed BSPP are assumed to be (165 °C, 7.0 bar), (95 °C, 0.85 bar) and (95 °C, 0.85 bar) respectively. (This assumption is based on the work of Almanza & Lentz (2001) [30] who had studied the production of electricity at low powers with parabolic troughs using saturated steam at 165 °C and 7.0 bar pressure). Assuming a 50% moisture content in the liquid-vapor mixture that exit from the expander (engine), the corresponding enthalpies of the working fluid at positions 1 to 3 of the cycle are 2766.43 kJ/kg, 1533.24 kJ/kg and 398.07 kJ/kg respectively (from water-steam tables [43]). Applying equation (3.73a), the thermal cycle efficiency η_{cycle} is calculated to be 52.07%; substituting into equation (3.74) and assuming η_E = 50% & η_{gen} = 90%, the overall efficiency of the PCU η_{pcu} is determined to be 23.43%.

Using the above estimations and applying equation (3.68), the hourly heat addition $\dot{Q}_A$ needed by the steam boiler to enable the PCU to generate at the rated power P_{rated} of 20 kW_e is calculated to be 307.3 MJ. (Note: 20 kW_e produced in one hour is equivalent to an energy output Q_{output} of 72 MJ). Similarly, by substituting $\dot{Q}_E$ = 80 MJ/hr into equation (3.69), the corresponding hourly mass flux of steam $\dot{m}_s$ needed by the expander (engine) to generate at rated power is found to be 129.7 kg/hr (0.036 kg/s). Mechanical energy input into generator $\dot{Q}_E$ is obtained by dividing Q_{output} by η_{gen}.

The steam boiler in the Rankine cycle is consisted of a submerged heat exchanger (HX) in a water vessel. The HTF, usually a thermal oil, heats up in the collector field & cools down in the HX, producing vapor in the vessel. By equating the collector useful gain Q_u with the boiler heat addition Q_A, the oil temperature at boiler inlet T_{bi} that must be maintained for generation at rated power can be calculated by [44]:

$$q_u = \frac{Q_u}{A_a} = F_B F_R U_L \left(T_{bi} - T_{sat}\right) \tag{3.75}$$

$$F_B = \left[1 + \frac{F_R U_L}{\dot{m} C_p \left(exp\left(UA_B / \dot{m} C_p \right) - 1 \right)} \right]^{-1} \tag{3.75a}$$

where F_B is the boiler heat removal factor and UA_B is the overall heat transfer coefficient in the boiler HX. In this instance, assuming no heat losses occur between the boiler and the collector, T_{bi} & oil temperature at boiler outlet T_{bo} can be equated with the collector fluid outlet temperature T_{fo} & inlet temperature T_{fi} respectively.

By rearranging equation (3.27), the useful gain of the collector can be expressed as:

$$Q_u = \eta_i \cdot A_a \cdot I_a \tag{3.76}$$

And from equation (3.28), $Q_u = \dot{m} C_p \left(T_{fo} - T_{fi} \right)$

Similarly, the heat addition to the boiler can be expressed in terms of T_{bi} and T_{bo} as:

$$Q_A = \dot{m} C_p \left(T_{bi} - T_{bo} \right) \tag{3.77}$$

Thus, by setting up a mass & energy transfer balance between the collector and the steam boiler using equations (3.75), (3.76), (3.28) & (3.77), and substituting I_a with $I_{std,s}$ & $I_{std,pc}$ in equation (3.76), the optimal collector (aperture) area A_a needed for electricity generation at rated power under sunny & partly cloudy conditions can be determined. Based on the evaluated optimal A_a, the suitable boiler's T_{bi} & T_{bo}, and the corresponding range of fluid mass flux required to keep them constant for steady boiler operation can be established.

3.5 Construction and Installation of Solar Parabolic Trough at SERT

As mentioned previously in Chapter 1, the School of Renewable Energy Technology (SERT) installed a 50-m long parabolic trough collector at the Energy Park (referred to as "EPC") to promote research on high temperature solar thermal technology. This collector is considered to be the largest industrial-scale solar parabolic trough ever to be built and tested under real solar conditions in Thailand. The EPC forms the main part of the solar trough test facility at the SERT that includes a feedwater loop and a data acquisition system to monitor the thermal performance of the collector (Figure 32).

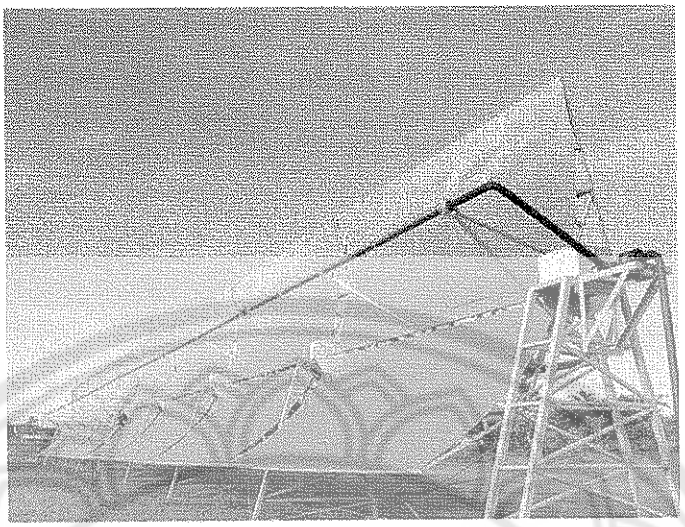

Figure 32 The complete EPC at the Energy Park

The first step in the construction of the solar trough EPC begins with a study of the physical characteristics of the LS-2 and LS-3 (LUZ system) collectors used in the commercial SEGS plants. Whenever possible, some aspects of these characteristics have been incorporated in the design of the EPC. Table 8 highlights some similarities between the commercial LS-2 & LS-3 collector systems and the EPC at the Energy Park. The solar trough EPC is designed to consist of eight elements or modules connected in series to form a complete solar collector assembly. Each module is comprised of the following: 2 end-plates, 6 pairs of cantilever arm, 1 torque-box central frame, 10 pieces of trough-base and 3 receiver supports (Figure 33). Each linear receiver is consisted of a cylindrical absorber pipe and a glass cover.

Table 8 Main physical parameters of the LS-2, LS-3 and EPC

Collector type	LS-2	LS-3	EPC
Aperture length (m)	47.1	99.0	48.0
Aperture width (m)	5.00	5.76	5.00
Aperture area (m^2)	235.5	570.2	240.0
Concentration ratio (geometric)	22.4	26.1	22.4
Focal distance (m)	1.49	1.71	1.71
Rim angle (degree)	79.9	80.2	72.3
Absorber diameter (m)	0.07	0.07	0.07

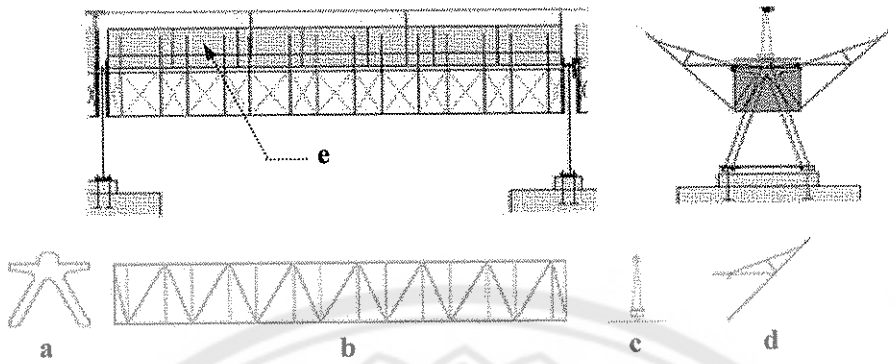

Figure 33 Each EPC collector module is consists of (a) endplates; (b) torque-box central frame ; (c) receiver supports; (d) cantilever arms; and (e) trough-base

The reflective surface of the trough is composed of 80 highly polished anodized aluminum facets mounted on the trough-base. The design of the central frame is based on the "torque-box" model of the advance European-design "EuroTrough" which have shown to provide better structural rigidity compared to the LS-2 and LS-3 collectors [45 & 46] (Figure 34). Once the design of the EPC has been determined, the next step is to consider the choice of material for the components of the collector assembly. Here again, reference is made to the successful experience of the commercial LS-2 and LS-3 collectors. However, the final decision is usually based on a compromise between cost, availability and acceptable quality. Table 9 shows a list of the essential materials that were used to fabricate the main components of the EPC module.

Table 9 List of material for main components of EPC module

Component	Material
Absorber pipe	Carbon steel pipe
Glass cover	Borosilicate glass pipe
Receiver support	Anodized aluminum
Reflective surface	Outdoor grade, 0.5 mm thick anodized aluminum, reflectivity = 93%
Cantilever arm	3 mm thick, 38 mm square tubular mild steel
Torque-box central frame	3 mm thick, 38 mm square tubular mild steel
Trough-base	3 mm thick aluminum sheet

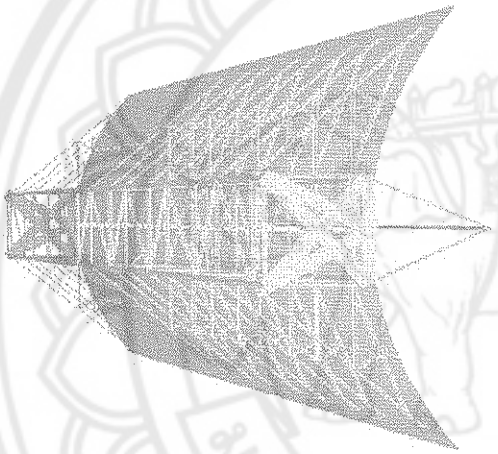

Figure 34 Torque-box central framework

Figure 35 Setting the parabolic curve

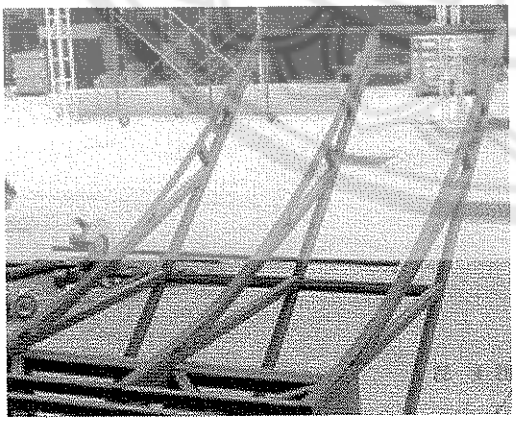

Figure 36 Cantilever arm

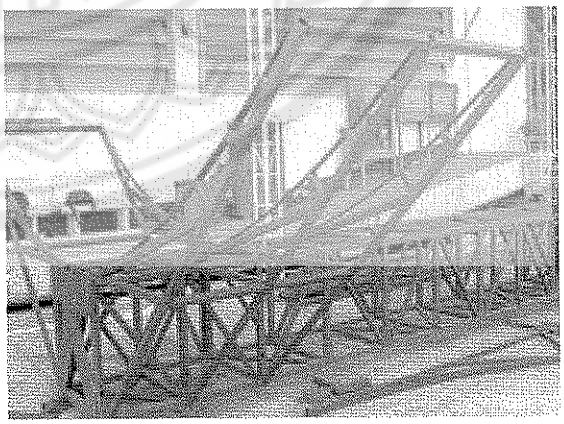

Figure 37 Assembly of cantilever arm & framework

Fabrication of the EPC can begin once the selection of material has been finalized. A simple jig is fabricated based on the standard equation of the parabola. Once the aperture width and the focal distance of the parabolic trough are determined, the shape of the parabolic curve can be formed (Figure 35). Next, the cantilever arms supporting the trough and the torque-box framework are constructed and assembled (Figure 36 & 37). This is followed by the placement of the trough-base and reflective surface, and the partially-completed module is now ready for receiver alignment testing (Figure 38). If the receiver is well-aligned, an intense glow of light can be seen on the underside of the receiver (Figure 39). On a sunny day, it is possible for the temperature at the receiver to reach up to 175 $^{\circ}$C or higher (Figure 40).

When all the individual modules are ready, they are transported to the Energy Park at SERT and installed on-site (Figure 41). The fully-assembled solar trough is oriented to operate on a horizontal north-south axis and tracks the sun by a mechanical drive, from east to west, at an angular velocity of 15° per hour. Water is used as the working fluid, and direct solar steam is obtained at the exit of the collector (Figure 42).

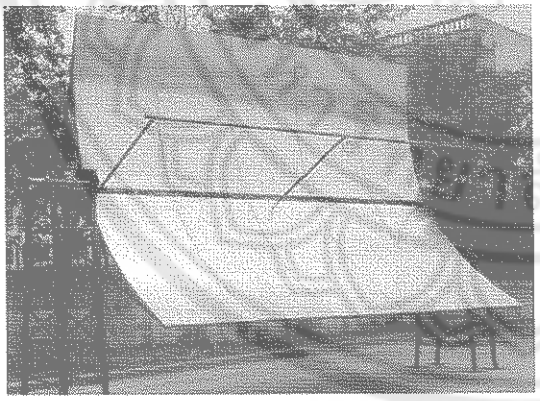

Figure 38 A partially-assembled module

Figure 39 Receiver under alignment testing

Figure 40 Temperature measured at receiver

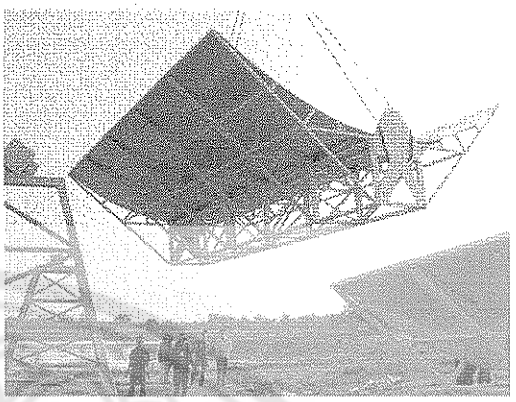

Figure 41 Installation of the EPC at SERT

Figure 42 Steam produced by the EPC collector

3.6 Data Collection and Measurements

The solar trough test facility is consisted of a closed-loop collector system where the outlet end of the EPC is connected to its inlet end in a continuous circulating flow manner. The steam or water-steam mixture that emerges from the collector is piped to two storage tanks of capacity 10 m^3 each before it is pumped back into the collector again. A computerized data monitoring and acquisition system supplied and installed by Yokogawa Electric Corporation makes up the rest of the solar trough test-loop as shown in Figure 43. Table 10 shows a list of instruments of the monitoring system and the parameters they measured. The location and installation of the pyrheliometer, flowmeter, temperature and pressure transmitters are illustrated by Figures 44-49.

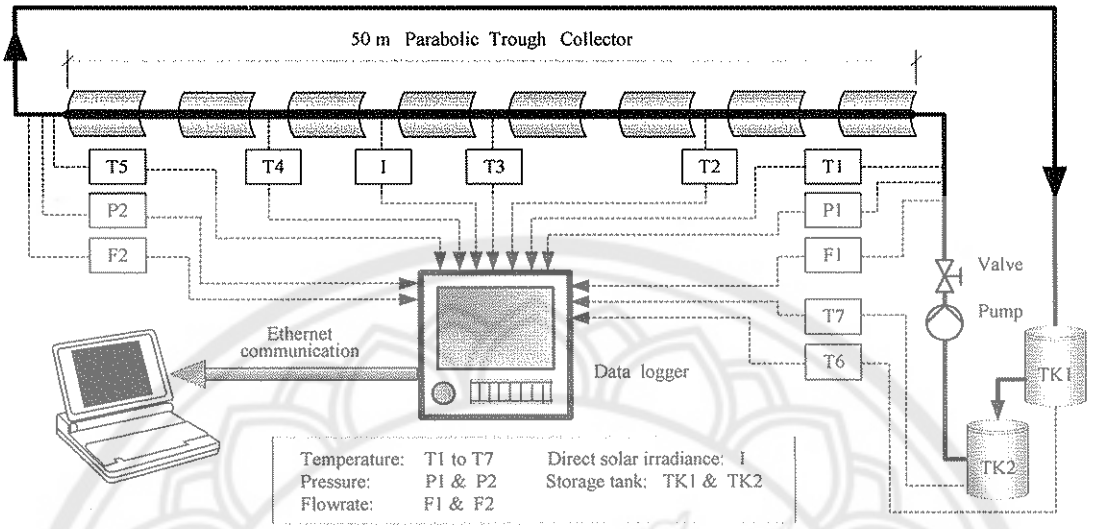

Figure 43 Solar trough test-loop with computerised data monitoring and acquisition system

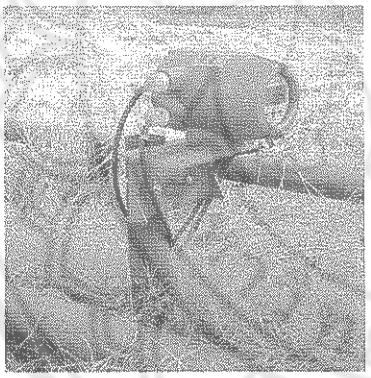

Figure 44 Magnetic flowmeter (F1)

Figure 45 Pressure sensor (P1)

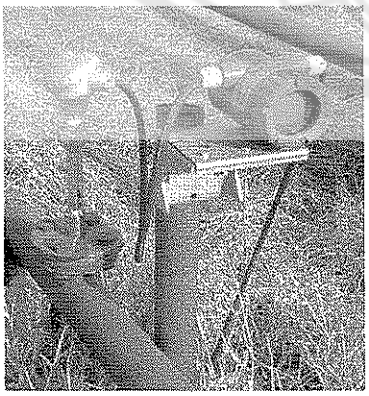

Figure 46 Temperature sensor (T1)

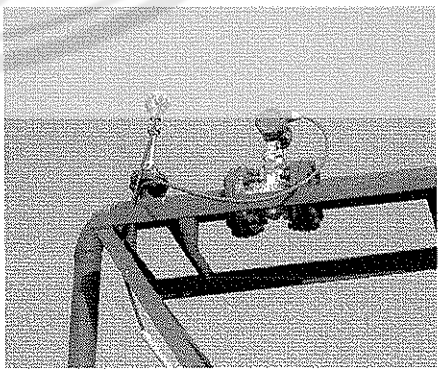

Figure 47 Vortex flowmeter (F2)

Table 10 Instruments of the monitoring system and parameter measured

Instrument	Manufacturer	Model	Set	Parameter measured
Pyrheliometer	Kipp & Zonen	CH1	1	Direct solar irradiance
Magnetic flowmeter	Yokogawa	AXFA14G	1	Inlet flow rate
Vortex flowmeter	Yokogawa	DY	1	Outlet flow rate
Temperature transmitter	Yokogawa	YTA	7	Temperature
Pressure transmitter	Yokogawa	EJA510A	2	Pressure
Data recorder	Yokogawa	DX200	1	Data logging

All the instruments are new and were pre-calibrated by the manufacturers. The accuracy of the pyrheliometer is +/- 0.5% while the accuracies of the flowmeters, temperature & pressure transmitters are +/- 1.5%, +/- 1.0% & +/- 1.0% respectively.

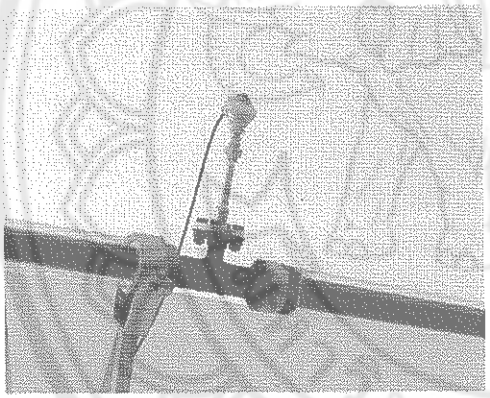

Figure 48 Temperature sensor (T2)

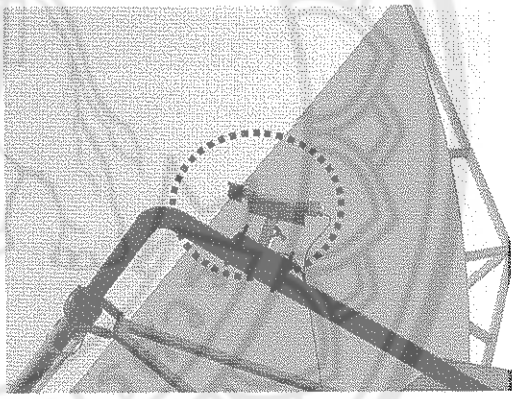

Figure 49 Pyrheliometer